SCANNING VOL. 35, 141–168 (2013)

Is Scanning Electron Microscopy/Energy Dispersive X-ray Spectrometry (SEM/EDS) Quantitative?

Dale E. Newbury* and Nicholas W. M. Ritchie

Surface and Microanalysis Science Division, National Institute of Standards and Technology, Gaithersburg, Maryland

Summary: Scanning electron microscopy/energy dispersive X-ray spectrometry (SEM/EDS) is a widely applied elemental microanalysis method capable of identifying and quantifying all elements in the periodic table except H, He, and Li. By following the "*k*-ratio" (unknown/standard) measurement protocol development for electron-excited wavelength dispersive spectrometry (WDS), SEM/EDS can achieve accuracy and precision equivalent to WDS and at substantially lower electron dose, even when severe X-ray peak overlaps occur, provided sufficient counts are recorded. Achieving this level of performance is now much more practical with the advent of the high-throughput silicon drift detector energy dispersive X-ray spectrometer (SDD-EDS). However, three measurement issues continue to diminish the impact of SEM/EDS: (1) In the qualitative analysis (i.e., element identification) that must precede quantitative analysis, at least some current and many legacy software systems are vulnerable to occasional misidentification of major constituent peaks, with the frequency of misidentifications rising significantly for minor and trace constituents. (2) The use of standardless analysis, which is subject to much broader systematic errors, leads to quantitative results that, while useful, do not have sufficient accuracy to solve critical problems, e.g. determining the formula of a compound. (3) EDS spectrometers have such a large volume of acceptance that apparently credible spectra can be obtained from specimens with complex topography that introduce uncontrolled geometric factors that modify X-ray generation and propagation, resulting in very large systematic errors, often a factor of ten or more. SCANNING 35: 141–168, 2013. †Published 2012 Wiley Periodicals, Inc.

Key words: elemental analysis, energy dispersive X-ray spectrometry, EDS, scanning electron microscopy, SEM, silicon drift detector, SDD, quantitative analysis, X-ray microanalysis, X-ray spectrometry

Introduction

Scanning electron microscopy with energy dispersive X-ray spectrometry (SEM/EDS) is an elemental microanalysis technique widely applied across a broad range of the physical and biological sciences, engineering, technology, and forensic investigations (Goldstein *et al.*, 2003). Electron-excited characteristic X-ray peaks provide identification and quantification for all elements of the periodic table, with the exceptions of H, He, and Li, that are present as major constituents (arbitrarily, a concentration $C > 0.1$ mass fraction or 10 weight%), minor constituents ($0.01 \leq C \leq 0.1$ mass fraction), and trace constituents ($C < 0.01$ mass fraction) to a limit of detection (C_{DL}) typically in the range 0.001–0.003 mass fraction depending on the element of interest, the matrix in which it resides, and the instrument operating conditions. With tens of thousands of SEMs equipped with EDS systems operating worldwide, many thousands of elemental identifications and concentration determinations are reported daily. Qualitative and quantitative X-ray microanalysis techniques in the SEM have evolved as a natural progression of the technique of "electron probe X-ray microanalysis (EPMA)" developed by Castaing ('51). EPMA is a rigorous measurement method that follows strict requirements for specimen preparation and for instrument operating conditions, and EPMA quantitative analysis results are subject to a well-defined error budget that enables rigorous estimates of precision and accuracy

*Address for reprints: Dale E. Newbury, Surface and Microanalysis Science Division, National Institute of Standards and Technology, Gaithersburg, MD 20899
E-mail: dale.newbury@nist.gov

Received 10 May 2012; Accepted with revision 29 June 2012

DOI 10.1002/sca.21041
Published online 9 August 2012 in Wiley Online Library (wileyonlinelibrary.com)

(Goldstein *et al.*, 2003). SEM/EDS is capable of quantitative analysis with accuracy and precision equivalent to wavelength dispersive spectrometry (WDS) analysis (Ritchie *et al.*, 2012). However, SEM/EDS is often performed under much less controlled measurement conditions, especially with regard to the condition of the specimen and the location of the beam on topographically complex surfaces. A reasonable question to ask is therefore: is SEM/EDS quantitative? This article will attempt to answer this question with a review of the state of quantitative X-ray microanalysis as performed with SEM/EDS, beginning with a brief review of EPMA, which is widely and justifiably regarded as the "gold standard" of elemental microanalysis.

Development of Quantitative X-ray Microanalysis: Wavelength Dispersive X-ray Spectrometry

Quantitative electron-excited X-ray microanalysis was first demonstrated by Castaing ('51) in the electron probe X-ray microanalyzer (EPMA) that he developed using WDS for X-ray intensity measurements. Castaing recognized that the efficiency of the WDS was a very complex function of photon energy due to the nature of the diffraction process, the need for different diffraction crystals to cover the photon energy range of analytical interest, and the variable solid angle with photon energy, making the quantitative comparison of X-ray intensities between different elements impractical due to the very large uncertainties that resulted. To overcome this severe limitation, Castaing introduced a simple, elegant measurement solution: the "*k*-ratio" measurement protocol in which the same X-ray peak was measured for the specimen ("spec") and a standard ("std") containing a known amount of that element under identical instrumental conditions (generally in immediate sequence) to form a ratio of the X-ray intensities, I_x:

$$k = I_{spec}/I_{std}. \quad (1)$$

Because the instrumental efficiency was identical for both measurements, this factor canceled quantitatively in the ratio. Castaing noted that this "*k*-ratio" was proportional to the ratio of mass concentrations between the unknown and the standard. He developed the physical basis for quantification by identifying a series of multiplicative "matrix correction factors" applied to the *k*-ratio, which accounted for the compositionally dependent effects of electron scattering, electron energy loss (stopping power), primary X-ray generation, X-ray absorption during propagation through the material, and secondary X-ray generation resulting from inner shell ionization by the photoelectric absorption of the primary characteristic and bremsstrahlung (continuum) X-rays by atoms of the sample. In its modern construction, the formula for the calculation of relative concentrations has the form:

$$C_{spec}/C_{std} = kZAFc, \quad (2)$$

where Z is the "atomic number correction," A is the "absorption correction," and F and c are the "secondary fluorescence corrections" for characteristic (F) and bremsstrahlung or continuum (c) radiation. As presented in Equation (2), Castaing's approach separates the instrumental measurement science of the *k*-ratio from the physical description of the generation and propagation of X-rays embodied in the matrix corrections.

The WDS separates the X-ray photon energies on the basis of Bragg diffraction from a crystal or artificial layered material, a process that is sharply defined in angle. To maximize collected intensity, the WDS is constructed as a focusing device whose transmission efficiency depends critically on precise positioning of the X-ray source (the focused electron-beam impact on the specimen), the diffracting crystal, and the X-ray detector (gas ionization chamber). The focusing properties of the WDS (mounted in the so-called "vertical geometry") are so sharply defined at the specimen that a few micrometers displacement of the specimen along the optic axis from the ideal level causes a significant loss in measured intensity. Reproducible WDS measurement of X-ray intensities requires precise specimen positioning, a condition achieved in the EPMA by means of a fixed optical microscope with an extremely shallow depth-of-focus positioned to be in exact focus at the same position as the WDS. Moreover, to satisfy the extremely limited WDS focal volume as the specimen was moved laterally, it was recognized that the specimen was required to be optically flat. A flat surface was also found to be critical because Equation (2) implicitly requires that the only reason that the X-ray intensity for an element differs between the specimen and the standard is that the composition is different. Geometrical structures such as scratches with dimensions on the micrometer scale similar to the electron interaction volume can significantly modify the generation and/or propagation of X-rays and introduce a large and unpredictable error component (Yakowitz, '68; Goldstein *et al.*, 2003). WDS microanalysts quickly learned that the only useful X-ray measurements were careful measurements with a well-prepared, optically polished specimen/standard suite.

The accuracy achievable by WDS analysis following the *k*-value measurement protocol with matrix corrections is illustrated by the relative error histogram in Figure 1 (Yakowitz, '75). To construct this histogram, materials of known composition (determined by independent bulk chemical analysis) that were demonstrated to be homogeneous on a

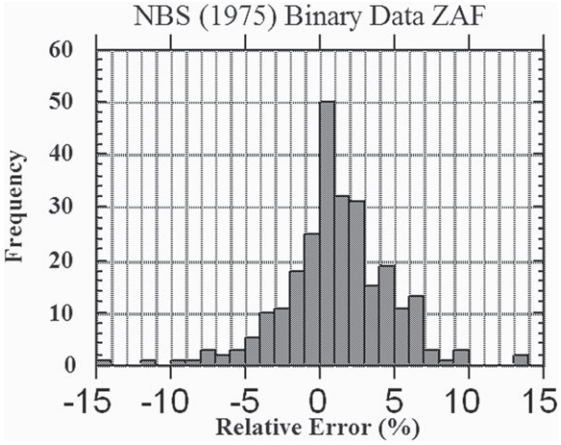

Fig 1. Error distribution for quantitative X-ray microanalysis with WDS *k*-ratio measurements and ZAF matrix corrections (NBS/NIST 1975 model; after Yakowitz, '75).

micrometer scale (as determined with extensive sampling by electron-beam X-ray measurement) were analyzed with the method of Equation (2) using pure elements and simple compounds (e.g., FeS_2 for S) as standards. The *k*-ratios were measured to a high degree of precision ($\sigma_{rel} \approx 0.5\%$ or less) so that the random counting statistics portion of the error budget is a small component of the distribution in Figure 1, which mostly depends on the systematic errors inherent in the particular matrix correction procedure applied. All of the elements measured for Figure 1 were present as major constituents. The relative errors for Figure 1 were calculated as

$$\text{Relative error} = [(\text{Measured} - \text{True})/\text{True}] \times 100\%. \quad (3)$$

By this definition, a positive relative error represents overestimation of the true (reference) concentration while underestimating produces a negative relative error. The error distribution in Figure 1 is approximately symmetrical about zero relative error and can be described as having a standard deviation of 2.5% relative error, so that approximately 95% of the analytical results fall within ±5% relative of the true value. Subsequent development of the matrix correction procedures by numerous workers over the ensuing 50 years have further narrowed this error distribution (e.g., Pouchou and Pichoir, '91) so that a reasonable estimate of current performance from their work is that 95% of analyses should fall within ±2.5% relative of the true value.

Development of Quantitative X-ray Microanalysis: Energy Dispersive X-ray Spectrometry with Si(Li)-EDS

The development by the radiation detection community in the 1960s of the semiconductor energy dispersive X-ray spectrometer (EDS) based on lithium-drifted silicon thick-crystal technology [Si(Li)-EDS] led to the first implementation of such a device on an electron-beam column by Fitzgerald *et al.*, ('68). EDS provided an important advance over WDS because the entire excited X-ray spectrum from a threshold of ~100 eV (current performance) to the Duane–Hunt limit of the X-ray bremsstrahlung set by the incident electron-beam energy (maximum value typically 30 keV) was now recorded in every EDS measurement. Having the complete X-ray spectrum enabled a full qualitative analysis to identify the elements present at every analyzed location. The time penalty for complete WDS scanning of the entire photon energy range of interest is such that, even with modern highly automated computer-controlled WDS systems, it is not common practice to perform a full qualitative analysis at every location sampled by the electron beam. EDS thus enabled a new level of qualitative microanalysis whereby the analyst did not risk failure in fully identifying major and minor constituents that might be encountered unexpectedly within a heterogeneous material, a situation that frequently exists given the microstructural complexity of many unknowns.

Quantitative EDS analysis following the *k*-ratio protocol was quickly demonstrated through the efforts of numerous researchers, including Reed and Ware ('72), Schamber ('73), Lifshin *et al.* ('75), Fiori *et al.* ('76), and numerous others. Accurate extraction of characteristic peak intensities from the bresmsstrahlung background and from modest peak interferences was demonstrated through tools such as spectral filtering followed by multiple linear least squares (MLLS) fitting with experimentally measured peak references (Schamber, '73). An example is given in Table I (Newbury, 2000) of such an analysis of

TABLE I Analysis of NIST Standard Reference Material 482 (Cu–Au alloys) with Si(Li)-EDS and NIST-NIH DTSA (concentrations in mass fraction)

Cu (SRM value)	Analysis	Rel error (%)	Au (SRM value)	Analysis	Rel error (%)	Raw analytical total
0.198	0.198 ± 0.0022	0.0	0.801	0.790 ± 0.0023	−1.4	0.988
0.396	0.399 ± 0.0017	+0.8	0.603	0.594 ± 0.0027	−1.5	0.993
0.599	0.605 ± 0.0014	+1.0	0.401	0.402 ± 0.0033	+0.2	1.007
0.798	0.797 ± 0.0013	−0.1	0.201	0.199 ± 0.0043	−1.0	0.996

$1 - \sigma$ error in composition based upon net peak counts propagated through the matrix corrections; beam energy = 20 keV; CuKα and AuLα; standards: pure Cu and Au (Newbury, 2000).

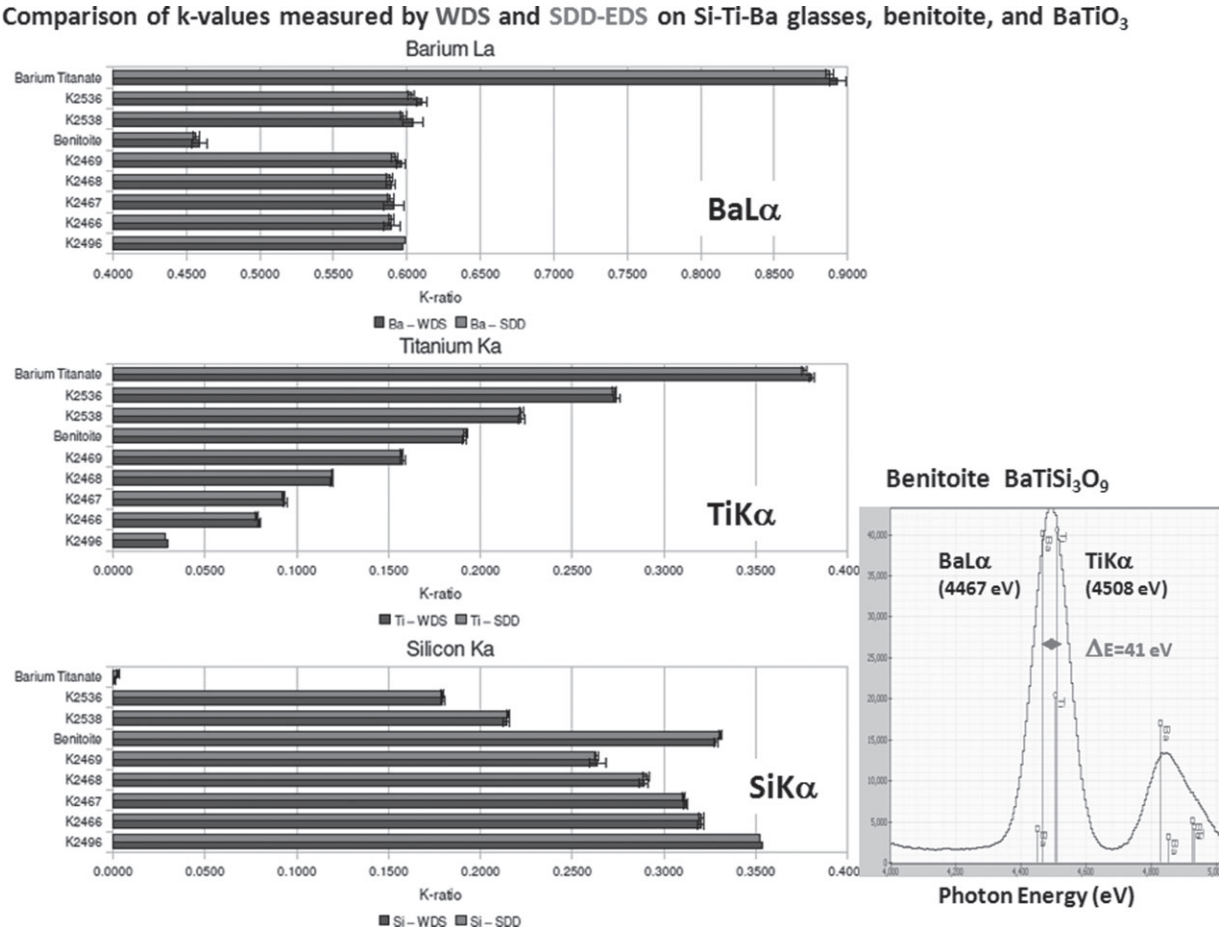

Fig 2. Comparison of *k*-ratios for Si, Ti, and Ba measured by WDS and SDD-EDS (Ritchie *et al.*, 2012).

the National Institute of Standards and Technology (NIST) Cu–Au Alloy Standard Reference Material 482 (Microanalysis Alloys) using Si(Li)-EDS spectra processed with the NIST-NIH Desktop Spectrum Analyzer (DTSA) software (Fiori *et al.*, '92) with MLLS and the "NIST ZAF" atomic number-absorption-fluorescence matrix correction procedure (Myklebust *et al.*, '79). The relative errors for all eight concentration determinations are less than 2% relative, which fit well within the WDS relative error distribution of Figure 1, and the analytical totals range from 98.8% to 100.7%.

Recent Advances in Quantitative X-ray Microanalysis: Energy Dispersive X-ray Spectrometry with SDD-EDS

The emergence of the silicon drift detector energy dispersive spectrometer (SDD-EDS) with its enhanced peak stability and greatly improved throughput compared to Si(Li)-EDS has provided the basis for an advance in analytical capability that challenges one of the long standing assumptions about EDS compared to WDS (Struder *et al.*, '98; Newbury, 2005a). Because of its relatively poor spectral resolution by a factor of ten or more, EDS has always been considered to be inadequate for quantitative microanalysis in critical situations when severe characteristic X-ray peak interference occurs. It has recently been demonstrated that SDD-EDS with MLLS peak fitting can match WDS for intensity (*k*-ratio) measurements even when severe peak interference occurs for major and minor constituents (Ritchie *et al.*, 2012). High-count SDD-EDS spectra with five million or more integrated spectral counts can be recorded in practical measurement times of approximately 100 s with a conservative detector counting strategy (e.g., a dead time of approximately 10%), which can serve as robust peak references for MLLS peak fitting. By comparison, Si(Li)-EDS spectra measured for the same time at the same spectrometer resolution at 30% dead time contain approximately 100,000 counts. Applying these statistically robust SDD-EDS peak references to MLLS peak fitting of similar high-count spectra of unknowns, X-ray peak intensities can be accurately extracted from the X-ray continuum background and from severely interfering peaks. An example is shown in Figure 2 for the interference of the Ba

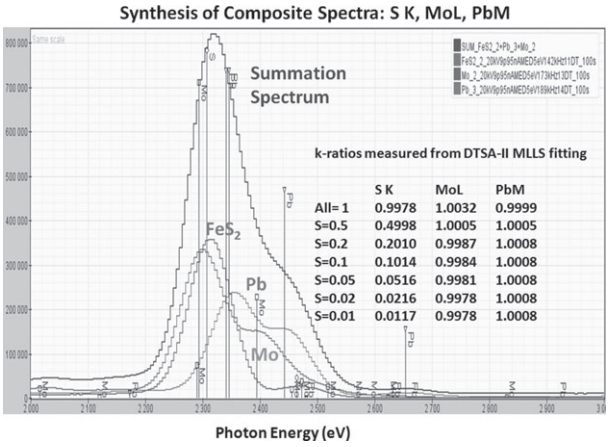

Fig 3. Extraction of k-ratios from spectra synthesized by adding experimentally measured pure element (Mo, Pb) and binary compound (FeS_2) spectra with DTSA-II spectrum math tools followed by MLLS peak fitting with different experimentally measured spectra as peak references.

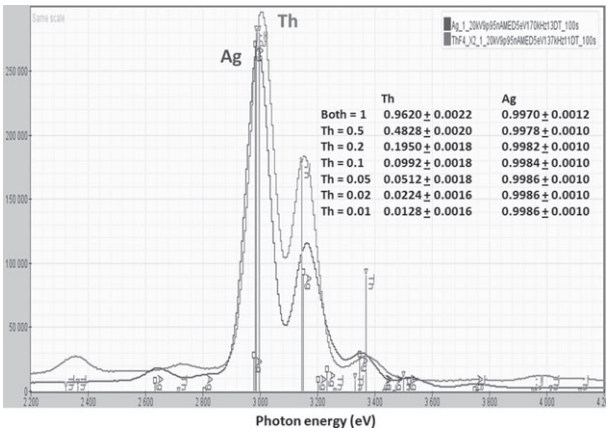

Fig 4. Extraction of k-ratios from Ag-Th spectra synthesized by adding experimentally measured pure element spectra with DTSA-II spectrum math tools followed by MLLS peak fitting with different experimentally measured spectra as peak references.

L_3-M_5 (Lα)–Ti K-L_3 (Kα) peaks, which are separated by 41 eV. A direct comparison was made of SDD-EDS and WDS k-ratios measured at the same locations for Si, Ti, and Ba on benitoite ($BaTiSi_3O_9$), barium titanate ($BaTiO_3$), and a series of Si–Ti–Ba glasses with various Ba/Ti ratios. The EDS spectra were processed with the recently developed NIST DTSA-II software engine (Ritchie, 2011). The k-ratios measured with SDD-EDS and WDS are consistent within counting statistics, even with a Ba/Ti mass fraction ratio above 20:1.

These interference studies can be extended indirectly to other peak interference systems for which suitable microscopically homogeneous materials are not available by using experimentally measured spectra of standards, which are then added in combinations using the spectrum calculator tools in DTSA-II. These summed spectra are then subjected to DTSA-II MLLS fitting using different standard spectra to serve as peak references. Examples of the results are shown in Figure 3 for the S K (2.307 keV), MoL 2.293 keV, and PbM (2.346 keV). All three spectra were combined, and then the S K intensity was decreased successively to 0.5, 0.2, 0.1, 0.05, 0.02, and 0.01 of the original level. The k-ratios recovered by MLLS fitting show excellent correspondence over the full range, with only a 12% relative error in the k-ratio for S K at a 100:1 reduction in intensity with interference from both MoL and PbM. A similar study is shown in Figure 4 for AgL-ThM, which not only features a separation of only 12 eV (AgLα = 2.984 keV; ThMα = 2.996 keV) for the principal peaks, but the full AgL-family and ThM-family peak structures overlap over an extended energy range as seen in the superimposed spectra. The errors are somewhat larger in this extreme overlap case, reaching a 28% relative error in the k-ratio for an Ag/Th ratio of 100:1. These results suggest that high-count SDD-EDS spectra can provide access even with severe overlaps to the upper trace concentration range (i.e., $C > 0.001$ mass fraction, 0.1 weight%).

The k-ratio measurement is the key step in achieving quantitative X-ray microanalysis by EDS with equivalent performance, in terms of the error histogram, to WDS. No matter which of the various matrix correction procedures is applied, accurate concentration results depend upon starting with accurate k-ratio measurements. Thus, being able to duplicate WDS k-ratios on elemental mixtures with strongly interfering peaks means that the same level of quantitative microanalysis accuracy available with WDS can now be achieved with SDD-EDS for major, minor, and upper trace level constituents. Further work is currently underway to better define the lower level of concentration that is practical with SDD-EDS, especially when peak interference occurs. Of course, as the concentration is lowered within the trace range, eventually a level will be reached where WDS is superior to SDD-EDS because of its superior resolution and its unique capability through the diffraction process of restricting the detector dead time to only the narrow energy band of the photons of interest, excluding dead time contributions from high-intensity peaks of major constituent elements. However, for a wide range of X-ray microanalysis problems involving major, minor, and upper trace level constituents, carefully following the k-ratio measurement protocol with SDD-EDS combined with control of the specimen geometry can provide robust, high confidence, and accurate results.

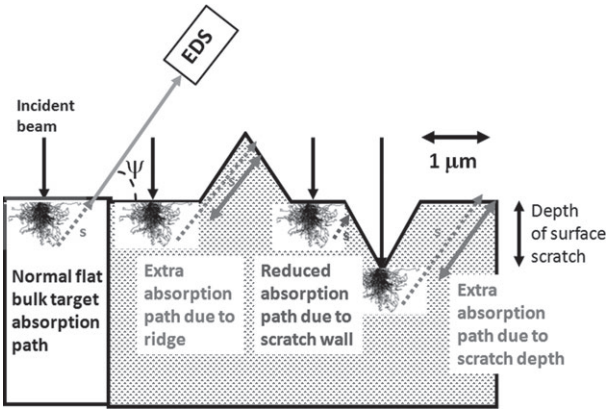

Fig 5. Schematic illustration of the effect of local topography on the X-ray path length to the detector. S = X-ray path length within specimen along detector axis; ψ = EDS detector takeoff angle, measured above the horizontal plane.

TABLE II Effect of surface condition on variability of measured X-ray intensity

Surface condition	AuMα C.V. (%)	σ (%)	AuLα C.V. (%)	σ (%)
600 grit SiC	8.6	0.13	1.8	0.31
500 nm Al_2O_3	0.7	0.13	1.1	0.31
100 nm Al_2O_3	0.46	0.13	0.42	0.31

Beam energy = 20 keV; 20 measurement locations; σ = single point counting statistic = $n^{1/2}/n$; C.V. = coefficient of variation = ($\sigma_{\text{distribution}}$/mean) × 100%; data from Yakowitz ('68).

"Best Practices" EDS Quantitative X-Ray Microanalysis

To achieve optimum results, the analyst must be aware of his/her responsibilities to perform robust SEM/EDS measurement science. While a complete list of "best practices" for EDS quantitative X-ray microanalysis must include specific procedures appropriate to the particular SEM/EDS system in use, it is useful to consider the most important general issues.

The Condition of the Specimen

Early in the history of the development of quantitative X-ray microanalysis, it was realized that a critical issue affecting the error budget concerned the condition of the specimen surface. A "0th" assumption of the model for quantitative X-ray microanalysis expressed in Equation (2) is that the only reason the X-ray intensity measured for the unknown differs from the intensity measured for the standard is that the composition is different, and no other factor affects the X-ray intensity. "Geometric effects" are variations in the local specimen topography that modify the electron interactions such as backscattering, which affects total X-ray generation and the depth distribution. As illustrated schematically in Figure 5, geometric effects arising from local topographic structures such as ridges and scratches, even fine-scale features with micrometer dimensions similar to that of interaction volume, can lead to strong changes in X-ray emission, since photoelectric X-ray absorption follows an exponential law.

$$I/I_0 = \exp[-(\mu/\rho)\rho s], \quad (4)$$

where I_0 is the starting intensity, I is the intensity after passage through a path s, (μ/ρ) is the mass absorption coefficient for the particular composition, and ρ is the density. Low-energy photons below 4 keV in energy are especially susceptible to such absorption path length effects.

The issue of what constitutes a sufficiently flat specimen to avoid geometric effects was considered by Yakowitz ('68), who examined the impact of surface roughness on the variance in the measured X-ray intensity for various pure metals and alloys by interrupting the metallographic grinding and polishing sequence after each step. Table II derived from his work shows the effects of specimen topography on measured WDS X-ray intensity after three different polishing stages as observed on pure gold, which provides both high-energy (AuLα = 9.711 keV) and low-energy (AuMα = 2.123 keV) characteristic X-ray peaks for simultaneous measurement. Comparison of the coefficient of variation for a suite of 20 fixed-beam location measurements with the single measurement counting statistic showed that the specimen topography of the 600 grit (U.S. grading) surface significantly affected the measured intensity for both the high- and low-energy peaks, with the coefficient of variation greater by a factor of 6–60 than the relative standard deviation of the peak count. For the 500-nm diameter (nominal) alumina polish, the coefficient of variation was reduced to approximately three times the precision of the single measurement for the high-energy peak, while the 100-nm diameter (nominal) alumina polish was needed to achieve this correspondence for the low-energy peak. If even lower photon energies are considered, especially below 1 keV, then surface topography should be reduced further, to an amplitude below 20 nm, to minimize the influence of topographic effects.

Operation of the EDS System

Before commencing any EDS microanalysis campaign, the analyst should follow an established checklist with careful attention to the measurement science of EDS operation:

1. *Choosing the EDS time constant (resolution)*: Before the starting of any EDS measurement campaign, the choice of the EDS amplifier time constant (a generic term that may be locally known as "shaping time," "processing time," "resolution," "count rate range," "1–6," etc.) should be checked. There are usually at least two settings, one that optimizes resolution (at the cost of X-ray throughput) and one that optimizes throughput (at the cost of resolution). Confirming the desired choice of the time constant is absolutely critical when the EDS system is in a multiuser environment, since the previous user may have altered this parameter.
2. *Choosing the solid angle of the EDS*: The solid angle Ω of a detector with an active area A at a distance r from the specimen is

$$\Omega = A/r^2. \tag{5}$$

   If the EDS is mounted on a movable arm that can alter the detector-to-specimen distance, then the user must select a specific value for this distance for consistency with archived standard spectra if these are to be used in quantitative analysis procedures. Because of the exponent on the distance parameter r in Equation (5), a small error in r propagates to a much larger error in the solid angle and therefore in the measured intensity.
3. *Selecting a beam current that produces an acceptable level of system dead time*: X-rays are generated randomly in time with an average rate determined by the flux of electrons striking the specimen. The EDS system can measure only one X-ray photon at a time so that it is effectively unavailable if another photon arrives while the system is "busy" measuring the first photon, causing the second photon to be excluded from measurement and effectively lost (depending on the progress in measuring the first photon when the second photon arrives, the first photon measurement may be excluded as well). An automatic correction function measures the time that the detector is busy, and to compensate for possible photon loss during this "dead time," additional time is added at the conclusion of the user-specified time so that all measurements are made on the basis of the same "live time" so as to achieve constant dose. The level of activity of the EDS is reported to the user as a percentage "dead time," which increases as the beam current increases. The dead-time correction circuit can correct the measurement time over the full dead-time range to 60% or higher (Note that as a component of a quality measurement system, the dead-time correction function should be periodically checked by systematically changing the beam current and comparing the measured X-ray intensity with predicted). However, as the dead time increases and the arrival rate of X-rays at the EDS increases, "coincidence events" can occur when two X-rays enter the EDS spaced so closely in time that the pulse inspection function will not recognize the two X-rays as distinct events. Such coincidence creates a sum of the two photon energies, which results in an anomalous event incorrectly placed in the EDS spectrum (energy histogram). The coincidence event can involve any combination of characteristic and background photons, but the distortion of the spectrum that results from coincidence is most easily observed when two characteristic X-ray photons combine to produce a "coincidence peak." This effect is illustrated in Figure 6 for a sequence of spectra measured at increasing dead time showing the ingrowth of a series of coincidence peaks as the dead time increases. With the long pulses of the Si(Li) EDS technology, the pulse inspection function was effective in minimizing coincidence effects to dead times in the range 20–30%. With the much shorter pulses of the SDD-EDS technology, the pulse inspection function is less effective, requiring dead times in the range of 10% to minimize coincidence peaks. Even with this restriction on dead time, the SDD-EDS is still a factor of ten or more faster than Si(Li)-EDS for the same resolution. In summary, as a critical step in establishing a quality measurement strategy, the beam current (for a specific EDS solid angle) should be selected to yield a dead time of approximately 25% [for SiLi)-EDS] or 10% [for SDD-EDS] on a target where the excitation creates a high X-ray flux, such as pure Al or Si. This beam current can then be used for all measurements with reasonable expectation that the dead time will be within acceptable limits.
4. *Performing the EDS energy calibration*: If the energy calibration is not correct, then the X-ray peaks will appear in the wrong locations, and all forms of peak identification can be expected to suffer increased failures, and the subsequent peak intensity measurement may also be subject to increased error. The calibration procedure should be performed according to the manufacturer's specifications, the test spectrum (spectra) for this procedure should be archived, and the dated record of the calibration parameters stored as basic part of a best practices quality assurance plan. Since calibration usually makes use of two widely separated peaks, e.g. AlKα,β and CuKα, CuLα,β and CuKα, etc., the calibrated EDS should be checked for the peak accuracy for intermediate energies, e.g. TiKα and FeKα, as well as for peaks outside of the calibration energy range: e.g. low photon energy peaks such as C K and O K where nonlinear behavior can occur, as well as high photon energy peaks, e.g. PbLα.

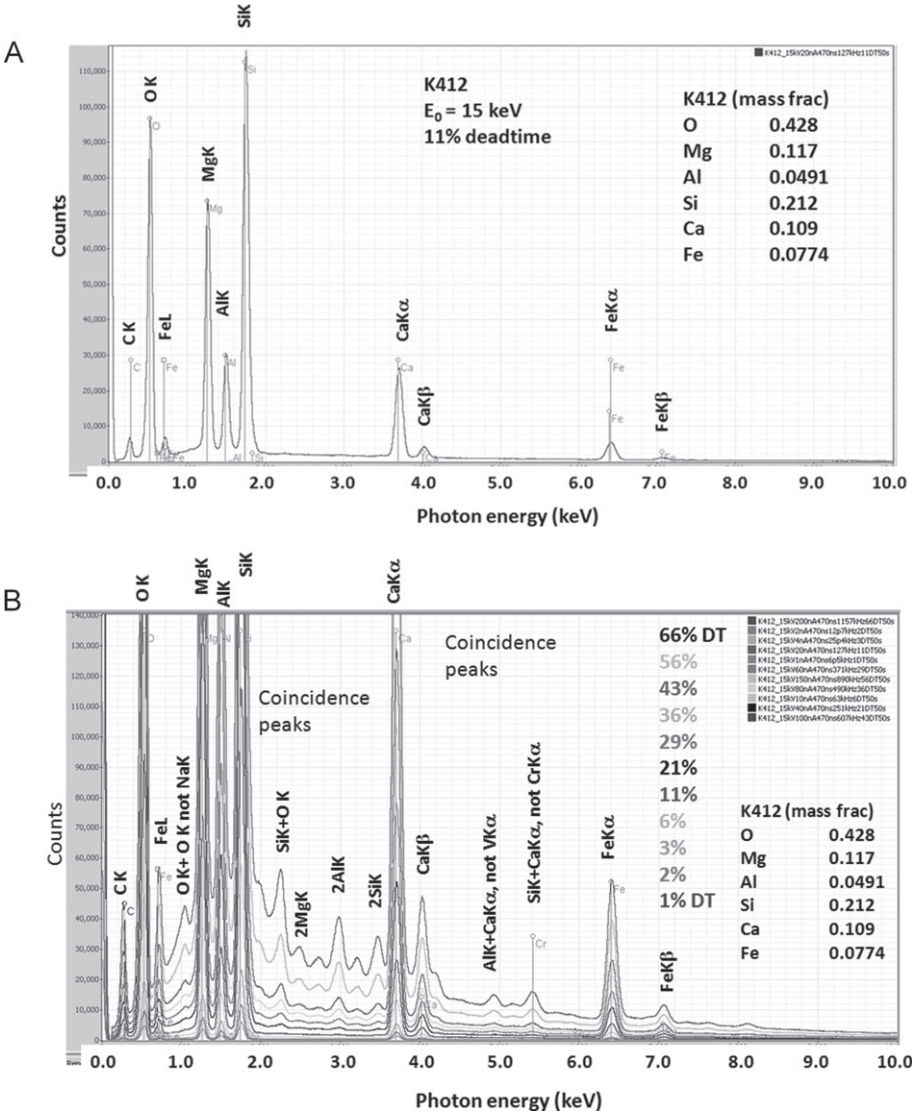

Fig 6. (A) SDD-EDS spectrum of NIST SRM 470 (glass K412) at a throughput of 6.5 kHz and a dead time of 1% (logarithmic display). (B) SDD-EDS spectra of SRM 470 (glass K412) over a wide range of throughput/dead time: from 6.5 kHz and 1% dead time; to 1157 kHz and 66% dead time. Note the ingrowth of the coincidence peaks such as 2MgK, 2AlK, 2SiK, etc.

5. *Recording adequate counts in the spectrum*: The confidence of peak identification in qualitative analysis and the precision of quantitative EDS X-ray microanalysis benefit by increasing the number of measured X-ray counts recorded in the spectrum. What constitutes an adequate number of X-ray counts depends on the particular analytical task. For a precise peak intensity measurement, the analyst might seek to record sufficient counts in a characteristic peak of interest above the local background so that the relative standard deviation is lowered to a desired precision, e.g. $\sigma_{\mathrm{rel}} = 1\%$, which corresponds to 10,000 counts above background. To detect a peak, it is common practice to consider that the detectable level (limit of detection) is established when the characteristic intensity integrated over the channels that define the peak exceeds three times the square root of the background intensity in those channels. Effectively, this is the background that would be measured in a blank, which corresponds to a material composed of the same major/minor elements without the element of interest. In EDS microanalysis practice a suitable blank is not usually available, so this background for the peak window is usually estimated for the measured spectrum either by background modeling constrained by measurements of the background in nearby regions where no peaks are observed or by MLLS fitting of the peak region. The minimum level for quantitative analysis, the so-called determination limit, is defined as a level that exceeds the standard deviation of the background by at least a factor of ten (Currie, '68).

The Software Tools

The modern SEM/EDS X-ray microanalysis system is typically implemented with a powerful, flexible, and extremely useful set of software tools to collect, interpret, and quantify X-ray spectra. These software tools have been developed by commercial vendors through many years of effort by numerous scientists and software engineers. Throughout its history, the EDS microanalysis instrumentation field has been at the forefront of incorporating into the laboratory the latest developments in computer hardware and software as well as employing algorithms based upon the continually improving understanding of the underlying physical basis of electron-excited X-ray generation, propagation, and detection. By making use of such commercial software tools for EDS spectral accumulation and the NIST-NIH DTSA or NIST DTSA-II software engines for MLLS peak fitting with matrix corrections for quantitative analysis, the excellent analytical performance presented in Table I and Figures 2–4 was achieved by carefully following the EDS *k*-ratio protocol. Virtually all commercial software platforms allow similar implementation of the *k*-ratio/matrix correction protocol, meaning that this level of analytical accuracy and precision should be available to all users of modern X-ray microanalysis systems. However, it must be emphasized that the analyst must recognize his/her responsibility to be a critical user of the software tools, understanding the limits of the particular analytical system at hand and not acting as an unquestioning consumer of the apparent authority of a slickly formatted output.

Challenges to SEM/EDS Credibility

The Perception of Quantitative X-ray Microanalysis with EDS

Despite the long history of SEM-EDS X-ray microanalysis, EDS quantitative analysis has generally been considered inferior to WDS quantitative analysis when highly reliable concentration results are needed. There appear to be at least three reasons for this state of affairs across the microanalysis community:

1. reliance on automatic peak identification for qualitative analysis and failure to recognize incorrect elemental assignments, which can occur even at the major constituent level but which are a frequent problem for minor and trace level constituents;
2. the domination of quantitative EDS microanalysis by standardless analysis procedures with broader and often undefined error histograms; and
3. the use of SEM/EDS to measure X-ray spectra of specimens with uncontrolled geometry (size, shape, local inclination), which introduces uncharacterized "geometric" errors with a magnitude much more significant than those noted above in the discussion of the surface finish of an ideal specimen. Indeed, the errors introduced by extreme specimen geometry can be so large as to render the quantitative analysis results virtually meaningless.
4. If the promise of the extraordinary quantitative X-ray microanalysis achievements demonstrated above by high-count SDD-EDS are to be realized across the SEM microanalysis community, it is critical to understand these issues and develop procedures to address the problems.

Is SEM/EDS Qualitative?

Before quantitative analysis by SEM/EDS can be attempted, the critical first step of qualitative analysis must be considered. Qualitative SEM/EDS analysis is the assignment of elements to the characteristic X-ray peaks recognized in the EDS spectrum. Often considered to be a trivial problem, achieving robust, high-confidence qualitative EDS analysis is, in fact, a challenge even at the level of major constituents, but the level of difficulty increases greatly as the concentration level decreases into the minor and trace levels. Virtually all qualitative EDS analysis is performed with a software tool variously called "automatic peak identification," "peak ID," or a similar name. When invoked, automatic peak identification applies a mathematical algorithm to locate and measure the photon energy of the characteristic peaks in the spectrum and then assigns elemental labels from a database of elemental X-ray energy information. Given the longevity of SEM/EDS systems and the on-going technical evolution of commercial automatic peak identification products currently in use, users may encounter various types of peak location strategy and mathematical rigor. Other differences are encountered concerning the degree of incorporation of X-ray physics information such as the occurrence of more than one X-ray family for an element or the extent to which minor X-ray family members within a peak series are considered. All of these factors bear on the success of the peak identification. While a powerful and useful tool, the automatic peak identification software should be considered to be only a starting suggestion, which the careful, skeptical analyst will inspect manually to determine which elemental assignments are valid. Obviously, a quantitative analysis based upon a faulty assignment of elemental identities is worthless. As with all software systems, there are usually critical choices of parameters for which the user is responsible.

Choosing automatic peak identification software parameters

Before considering the performance of automatic peak identification, several cautions must be raised concerning user-selectable parameters, which again comprise "best practices" issues.

1. *Peak threshold criterion*: A user-selectable threshold criterion on the size of a peak relative to the background counting statistics limits peaks to be considered for identification (alternatively, this parameter may be stated as a "minimum acceptable concentration" for identification). The threshold criterion influences the concentration level at which genuine peaks in the spectrum are considered in the final identification. Peaks corresponding to trace or even minor constituents may be ignored depending on the threshold setting. The threshold parameter can also influence the time during the spectral accumulation at which a peak identification solution is first displayed. If the parameter is set too low, the peak detection algorithm may trigger on statistical fluctuations in the background, creating false peaks and an apparent elemental identification solution that is not be stable. An example of this phenomenon is shown in Figure 7 for a sample of iron, where the identifications of small "peaks" in the specimen (W, P, Pd, Ag, Ca, and La in Fig. 7(A)) change markedly (Zn, As, Al, Au, and La in Fig. 7(B)) with only a 10% change in the integrated count. In fact, all of these apparent trace elements are manifestations of the statistical fluctuations in the continuum being misinterpreted as peaks by the peak-finding algorithm, with the exception of the La peak, common to both spectra, which is actually a misinterpretation of the FeKα Si-escape peak ($6.400 - 1.740 = 4.66$ keV; LaL$\alpha = 4.641$keV). Unfortunately, some analysts may be misled by the perceived authority of a software supplied solution, leading them to terminate the spectral accumulation too early and thus to "freeze in" an incorrect peak identification solution. It is thus important to be sure that sufficient counts have been accumulated to achieve a stable peak identification solution before proceeding to inspect the elemental results manually.
2. *Editing the allowed elements*: At least some commercial automatic peak identification systems allow the user to delete certain elements from consideration in the final peak identification solution because these elements are subject to frequent misidentification with that particular software system. Some of these systems even set default lists of "forbidden elements" that the user must actively act to defeat if these elements are to be considered by the automatic peak identification tool. An example of such a list embedded in a current software package is shown in Figure 8. Deleting elements from consideration is an extremely bad idea since this action only serves to cover up failings in the peak identification software, and this practice introduces the real hazard that if any of the "forbidden" elements is actually present in the specimen it will inevitably be ignored because it resides in the exclusion list.
3. *Editing the allowed X-ray family members*: Similarly, some automatic peak identification software systems permit the user to disregard certain minor X-ray family members that occur with low relative intensity, such as the (Ll (L_3-M_1), Lη (L_2-M_1), Mζ ($M_{4,5}$-$N_{2,3}$), and M_2-N_4. Again, this exclusion of information from consideration is likely to lead

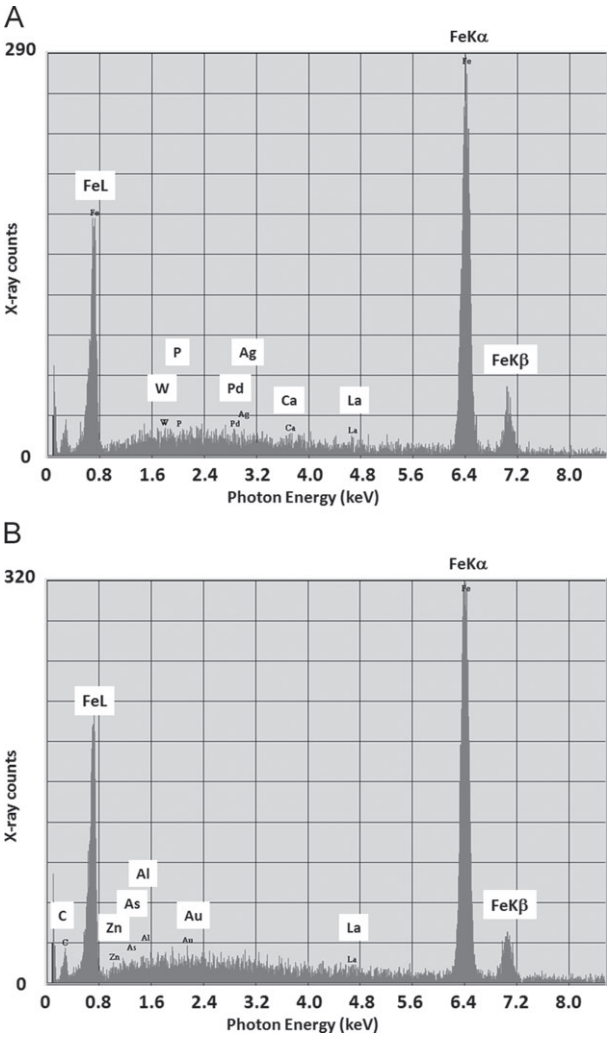

Fig 7. (A) Si(Li)-EDS spectrum of iron showing apparent trace element peaks marked by automatic peak identification during the spectrum accumulation. (B) Same spectrum after only 10% more counting time; note almost complete change in the trace elements with the exception of La (actually the FeKα escape peak).

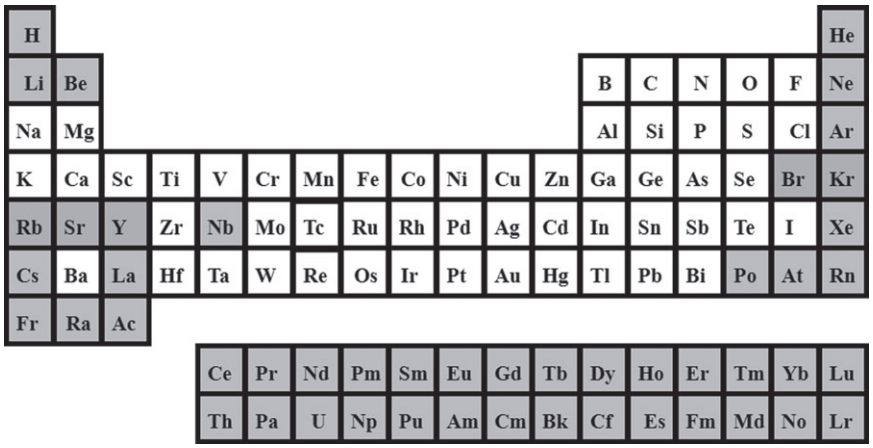

Fig 8. Example of a list of "forbidden" elements (element symbols grayed out) set as a default in a current software version.

to mistakes in peak identification. These low relative intensity family members actually produce detectable peaks that are well separated in energy from those of the principal family members, especially when the element in question is present as a major constituent. The danger is that if these minor family peaks are excluded from consideration, either from the database used for automatic identification or from the "KLM" lines used to aid manual qualitative analysis, then the unmarked peak(s) are likely to be assigned to an incorrect element that will be interpreted as occurring at the minor or trace level.

Peak misidentification

The careful analyst must be aware that even with "best practices" EDS operation and optimum choices made for the parameters listed above, there remains a significant possibility that peak misidentification may occur, even for major constituents that produce the highest relative intensity peaks in the spectrum and even with high counts (greatly in excess of 10,000 counts) in those peaks. Previous studies have reported egregious peak misidentifications for major constituents despite careful energy calibration and high spectrum counts, such as BrLα,β misidentified as AlKα,β, and PbMα,β misidentified as S Kα,β (Newbury 2005b). Table III lists some of the particular element pairs or multiplets that have been observed to produce peak misidentifications even at the level of major constituents. (Note: this list may not be complete). For older peak identification procedures that employed a peak-finding algorithm to locate a single channel to represent a peak and a lookup table of peak channel energies to locate matching values, it has been estimated that such egregious elemental misidentifications occur for approximately 3–5% of major constituent identifications when the entire periodic table (excluding H, He, and Li) must be considered. However this estimate is somewhat misleading, since the misidentification problem is not a random occurrence. For example, a system that misidentifies the BrL peak as AlK is highly likely to make this mistake for all Br-containing specimens. More recently developed peak identification software procedures that use the entire peak shape with MLLS fitting compared against library references and that also incorporate the physical rules for peak occurrence (e.g., K–L and L–M relationships for certain elements) have reduced the misidentification problem, but current work demonstrates that this very serious problem has not been eliminated from all current automatic peak identification software. Examples of peak misidentification blunders for major constituents with a current software system are

TABLE III Combinations of elements and characteristic peak families likely to produce misidentifications

Photon energy range (keV)	Element (energy)
0.390–0.395	N K (0.392); ScL (0.395)
0.510–0.525	O K (0.523); V L (0.511)
0.670–0.710	F K (0.677); FeL (0.705)
0.845–0.855	NeK (0.848); NiL (0.851)
1.00–1.05	NaK (1.041); ZnL (1.012); PmM (1.032)
1.20 to1.30	MgK (1.253); AsL (1.282); TbM (1.246)
1.45–1.55	AlK (1.487); BrL (1.480); YbM (1.521)
1.70 to1.80	SiK (1.740); RbL (1.694); SrL (1.806); TaM (1.709); W M (1.774)
1.90 to1.99	Y L (1.922); OsM (1.910)
2.00–2.05	PK (2.013); ZrL (2.042); PtM (2.048)
2.10–2.20	NbL (2.166); AuM (2.120); HgM (2.191)
2.28–2.35	S K (2.307); MoL (2.293); PbM (2.342)
2.40–2.45	TcL (2.424); BiM (2.419)
2.60–2.70	ClK (2.621); RhL (2.696)
2.95–3.00	ArK (2.956); AgL (2.983); ThM (2.996)
3.10–3.20	CdL (3.132); U Mα (3.170)
3.25–3.35	K Kα (3.312); InLα (3.285); U Mβ (3.336)
4.45–4.55	TiKα (4.510); BaLα (4.467)

Note this is only a partial list; more problematic elemental combinations are likely to be encountered.

TABLE IV EDS analysis of a high T_c superconductor crystal by standards-based *k*-ratio/ZAF and by two commercial standardless quantitative analysis protocols (concentrations in mass fraction)

Method	Y	Rel err (%)	Ba	Rel err (%)	Cu	Rel err (%)	Cu peak	Formula
True	0.133		0.412		0.286			$YBa_2Cu_3O_{7-x}$
k-ratio/ZAF	0.138	+3.8	0.411	− 0.2	0.281	− 1.7	CuKα	$YBa_2Cu_3O_{6.8}$
Standardless 1	0.173	+30	0.400	− 2.9	0.267	− 6.6	CuKα	$Y_2Ba_3Cu_4O_{10}$
Standardless 1	0.158	+19	0.362	− 12	0.316	+10.5	CuL	$Y_2Ba_3Cu_6O_{12}$
Standardless 2	0.165	+24	0.387	− 6.1	0.287	+0.35	CuKα	$Y_2Ba_3Cu_5O_{11}$
Standardless 2	0.168	+26	0.395	− 4.1	0.276	− 3.5	CuL	$Y_4Ba_6Cu_9O_{21}$

k-ratio/ZAF: NIST-NIH Desktop Spectrum Analyzer with multiple linear least squares peak fitting; standards for *k*-ratio/ZAF: Y (element); Ba (NIST K309 glass); Cu (element); $E_0 = 20$ keV.

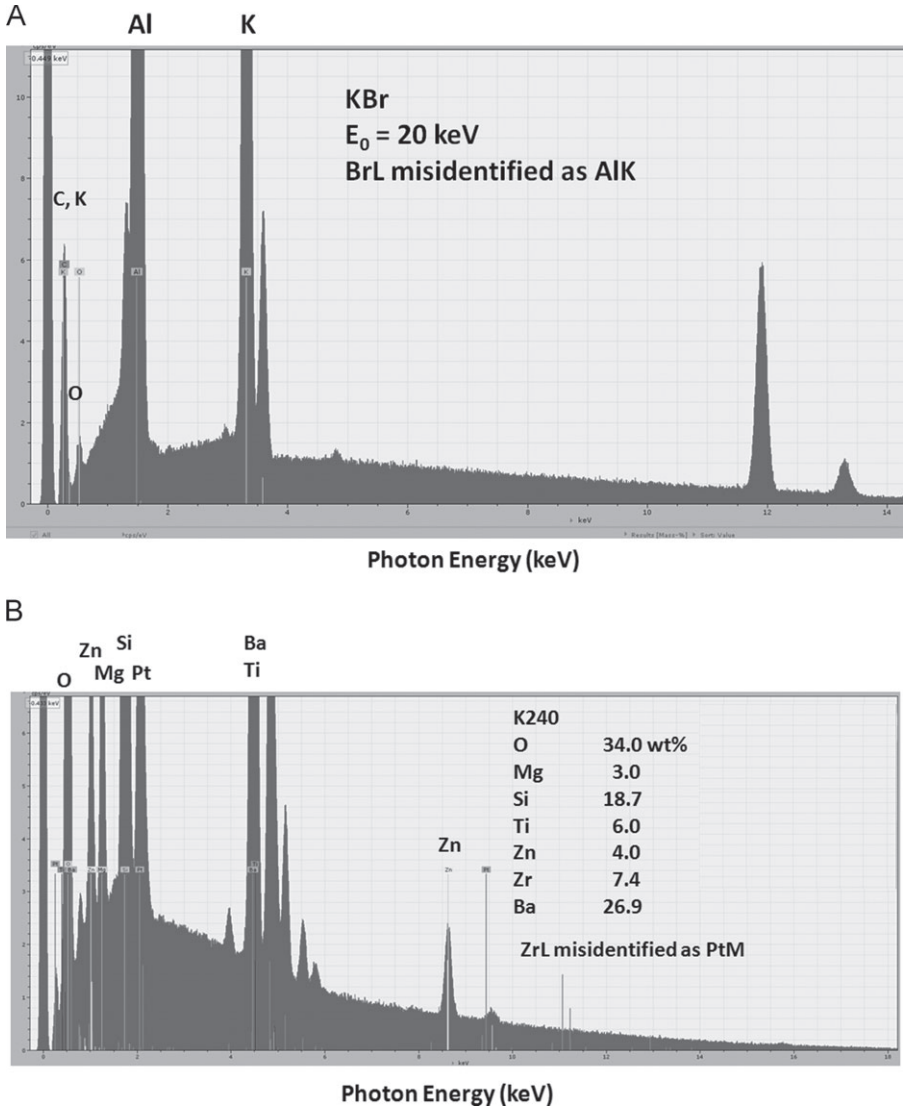

Fig 9. (A) SDD-EDS spectrum of KBr showing misidentification of BrL as AlK. (B) SDD-EDS spectrum of NIST glass K240 showing misidentification of ZrL as PtM.

presented in Figure 9, showing that some of the egregious problems observed in the 2005 study, e.g. AlK-BrL and ZrL-PtM, are still occurring. Some unexpected new problems are also observed, e.g. in Figure 10(A) the PbM- and L-family peaks are properly labeled in a sample of pure Pb, but in Figure 10(B) for a multielement glass containing a major lead constituent ($C = 0.417$ or 41.7 weight%) the PbM-family is labeled with a combination of S K and TcL while the prominent PbL peaks are completely ignored. This is

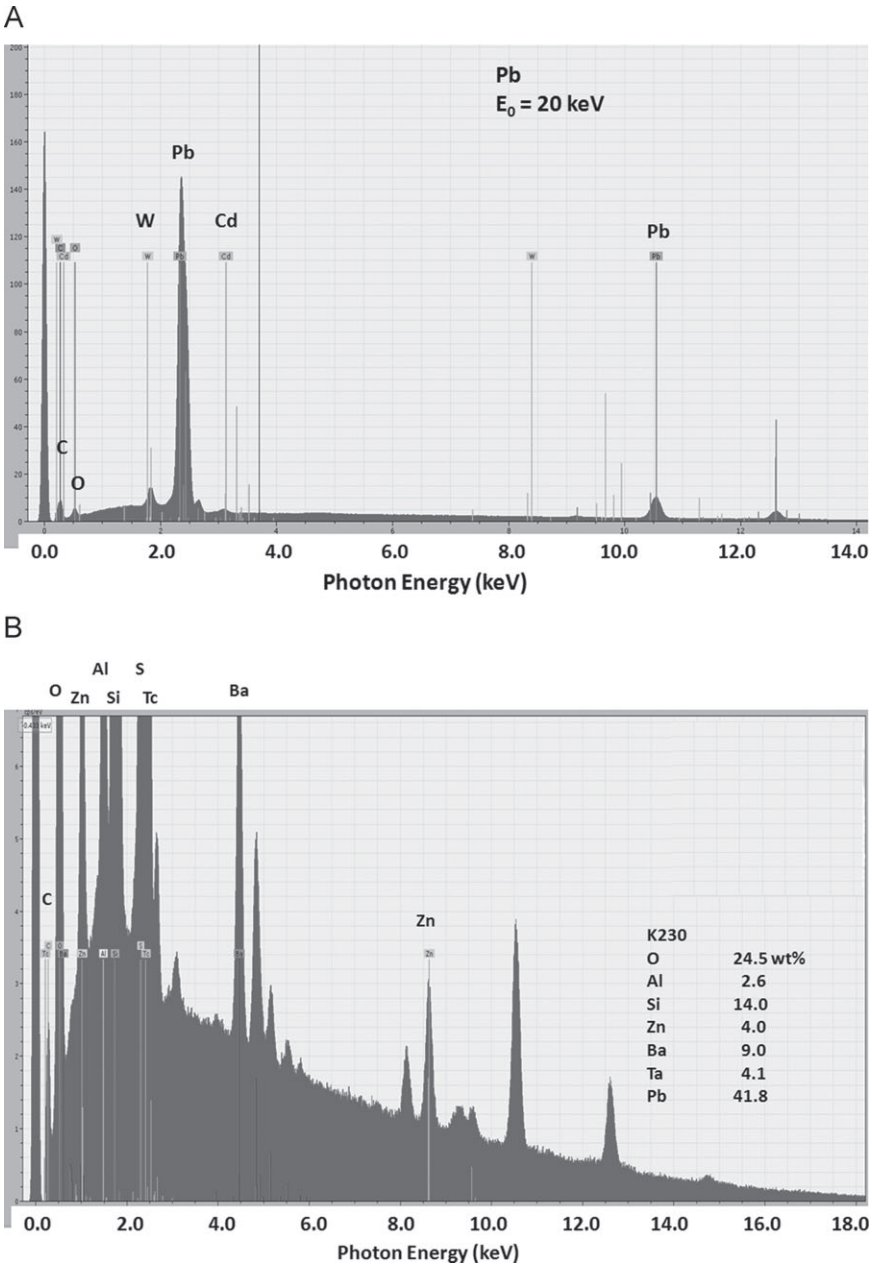

Fig 10. (A) SDD-EDS spectrum of high-purity Pb, showing correct labeling of the principal PbM and PbL peaks, but incorrect labeling of $PbM_{4,5}$-$N_{2,3}$ ($M\zeta$) as W M and PbM_2-N_4 as CdL. (B) SDD-EDS spectrum of NIST glass K230 showing misidentification of PbM as S K and TcL while ignoring the high-energy Pb L-family X-ray peaks.

a surprising observation, since the misadventures of automatic peak identification in any particular software system were found to be at least consistent in the earlier studies (Newbury 2005b, 2007, 2009). The inconsistency on pure lead and lead as a major constituent is therefore especially troubling. Note that the misidentification of Tc instead of Pb is especially suspicious since Tc is a highly radioactive artificially synthesized element (as is Pm), but remarkably the default list of "forbidden elements" for this particular automatic peak identification software system, illustrated in Figure 8, allows Tc while suppressing from consideration quite reasonable elements such as Sr, Br, and Nb.

The frequency of misidentifications by all generations of automatic peak identification software increases as the concentration of constituents drops into the minor and trace range (Newbury 2007, 2009). The problem of correctly identifying trace constituent peaks with high confidence and reliability is so difficult that some commercial systems are actually internally constrained to avoid any

identification in the trace range by ignoring peaks with a low peak-to-background, leaving this difficult and often critical characterization problem to the analyst.

Best practice in qualitative X-ray microanalysis

Major constituents. The automatic peak identification software provides results that are a useful first step, but the analyst must review each proposed elemental assignment. To avoid being misled by an egregious mistake from automatic peak identification of a major constituent, the careful analyst will always confirm the suggested peak assignments by performing manual peak identification using the available computer-aided analysis tools (e.g., KLM markers, peak fitting tools, etc.). Such software tools for manual identification must be further augmented by the user's understanding of the basic physics of X-ray production, propagation, and detection, which may not be incorporated in the automatic peak identification software. It is critical to know which characteristic peaks are available for a particular element at a given beam energy (excitation energy) and which can be accessed by modifying the beam energy within the limits of the SEM. A good strategy to begin a qualitative analysis is to select an incident beam energy of 20 keV, which will provide adequate excitation for peaks with photon energies as high as 12 keV. The confidence that can be assigned to a tentative elemental identification increases greatly when more than one X-ray peak or families of peaks can be identified. For elements with atomic numbers below 15 (phosphorus), only the Kα (K-L$_3$) X-ray peak will be available for identification since the Kβ (K-M) for low-Z elements is either nonexistent, very low relative intensity, or not resolvable from Kα with EDS. Starting with sulfur, and depending on the resolution performance of the EDS, additional family members will be resolved, e.g. Kβ, and for higher Z elements, the L-shell and M-shell X-ray families become available. The presence of K-shell X-rays above 4 keV for an element, e.g. TiKα, means that a corresponding L-shell X-ray is also excited and detectable. Similarly, L-shell X-rays above ~4.5 keV, e.g. BaLα, means that the corresponding M-shell X-ray peaks are also available. Studying the EDS spectra of pure elements and simple binary compounds measured over a range of beam energies is extremely helpful for developing a practical understanding of this critical X-ray physics, which despite its value is not necessarily embedded in automatic peak identification software as the examples above demonstrate.

- With the practical knowledge gained from studying X-ray spectra, the analyst can also develop strategy to choose the beam energy to deal with especially difficult peak identification problems by ensuring adequate excitation for the peaks of interest, and possibly by choosing a more appropriate beam energy to optimize the measurement. Such strategy is especially important when complex specimens containing elements of low, intermediate and high atomic number are to be measured. A strategy of repeated measurements with two or more beam energies may be required. For example, a higher beam energy may be appropriate to excite an additional X-ray families for elements of intermediate and high atomic number to increase the degree of confidence in the peak identification as noted above. However, an understanding of X-ray absorption is important when dealing with low photon energy peaks ($E < 1$ keV). Low-energy photons suffer higher relative absorption compared with photons with $E > 1$ keV, so that the depth of X-ray production in the target, which depends on the incident beam energy, can strongly influence the measured relative X-ray peak heights. Such high-absorption situations can be so severe as to lead to the apparent loss of even major constituents when they are represented only by low-energy peaks. This situation is illustrated for C in SiC measured with $E_0 = 20$ keV in Figure 11(A). C in Si represents a high-absorption situation because the Si L-shell absorption edges at ~100 eV are located below the energy of the C K characteristic X-ray at 282 eV. At $E_0 = 20$ keV, the self-absorption of the C in SiC reduces its intensity relative to the Si peak so much so that when the vertical display range is limited by the height of the Si peak, the C K peak is not visible as a distinct peak. The SiC specimen might be mistakenly interpreted as pure Si. Increasing the escape of C X-rays requires lowering the beam energy, so that with $E_0 = 3$ keV, the C K X-ray peak becomes readily apparent in Figure 11(B) as a major constituent.

Minor/trace constituents. The most challenging peak identification problem is that of achieving a robust level of confidence in identifying minor ($0.01 \leq C \leq 0.1$ mass fraction) and trace level ($C < 0.01$ mass fraction) constituents. Minor/trace constituent identification requires a careful, systematic approach that emphasizes comprehensive spectral study. First, each major constituent must be identified and all principal and minor X-ray family members of that element as well as all associated spectral artifacts (Si-escape peaks, coincidence peaks) must be located before proceeding to identify any remaining low relative intensity peaks as arising from minor constituents and eventually trace constituents. Examples of peak identification mistakes at the minor/trace level observed with current software products include

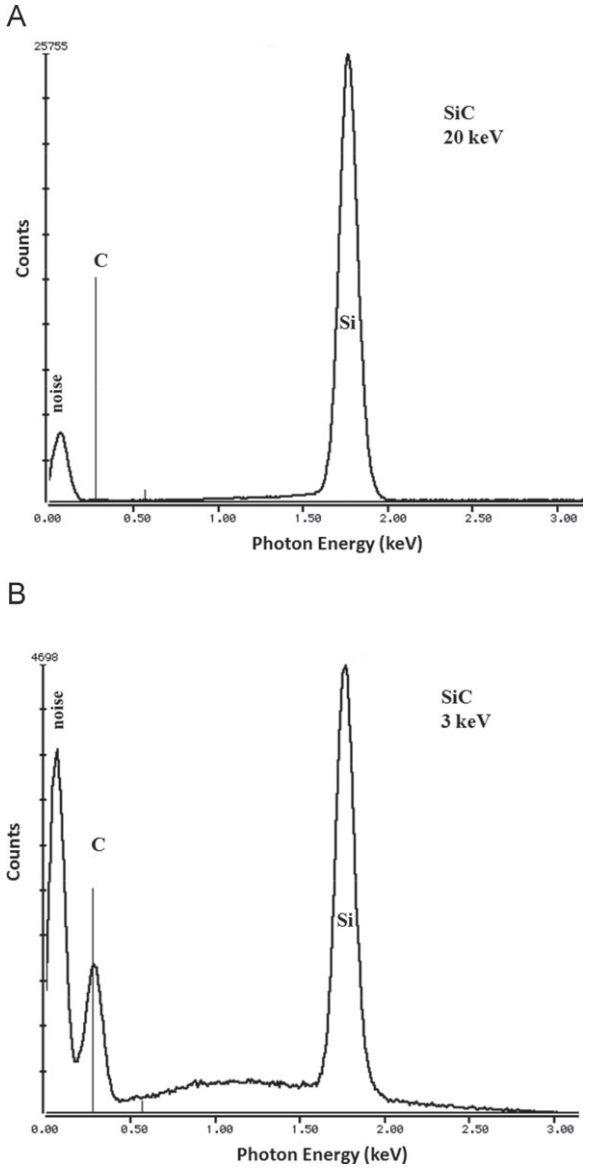

Fig 11. (A) Si(Li)-EDS spectrum of SiC with a beam energy of 20 keV. (B) Si(Li)-EDS spectrum of SiC with a beam energy of 3 keV.

1. Identifying false low level peaks by misinterpreting random statistical variations in the X-ray bremsstrahlung, as shown in Figure 7.
2. Failure to correctly assign minor X-ray family members of an identified major constituent is often followed by mislabeling those minor peaks as an incorrect element(s), as illustrated by the spectrum of pure Pb in Figure 10(A), where the $PbM_{4,5}$-$N_{2,3}$ ($M\zeta$) is mislabeled as W M and the PbM_2-N_4 as CdL.
3. Escape peaks and coincidence peaks are commonly misinterpreted by automatic peak identification systems because the rules governing these artifacts may not be embedded in the software procedures. Examples of misidentification of peak coincidence commonly encountered include the AlK coincidence identified as trace Ag and SiK coincidence identified as trace Sn shown in Figure 12(A) and (B). The misidentification of the Si escape peak is illustrated in Figure 13 for CrKα (5.411 keV), where the escape peak at 3.674 keV is misidentified as Ca K-L_3 (Kα) (3.690 keV). Note also the misinterpretation of the Cr K-shell sum peaks as BiL and SeL in this same spectrum.

The degree of confidence that can be placed in an elemental assignment inevitably declines as the concentration of a constituent decreases into the minor and trace ranges. The number of recognizable peaks available to make the identification is diminished because of the reduced counts in the minor X-ray family members. Improving the confidence in minor/trace constituent identification can only be achieved by investing longer spectral accumulation times to greatly increase the X-ray counts for low relative intensity peaks. With the new class of SDD-EDS detectors, large spectral integrals can be accumulated within acceptable time periods, e.g. 500 s or less to make possible more reliable minor/trace constituent analysis. However, the much faster pulses of the SDD-EDS lead to significant coincidence peak problems as illustrated in Figure 2. There is thus a conflict between the desire for high integral spectrum counts, obtaining those high counts as quickly as possible by exploiting the full throughput of SDD-EDS, and obtaining spectra with minimal artifacts. The SDD-EDS pulse coincidence problem leads to such significant spectral artifacts that it is recommended that throughput be restricted to dead time below 10% unless careful study of spectra justifies higher throughput, e.g. coincidence may occur, but not in the region of the spectrum where the true minor/trace constituent peaks of interest occur.

Standardless Quantitative Analysis

The second major issue affecting the status of EDS as a reliable quantitative analysis method is the widespread, indeed dominant, use of "standardless" quantitative analysis procedures. Probably 95% or more of the concentration results reported by SEM/EDS analysts are now derived from commercial "standardless" analysis software. The "standardless" protocol is an extremely attractive "one-button" procedure for use in the SEM/EDS measurement environment that apparently requires little intervention by the analyst. The EDS spectrum provides simultaneous (in energy, not time) measurement of the entire X-ray spectrum as excited in the SEM, in principle capturing all of the information needed for comprehensive compositional analysis in a single

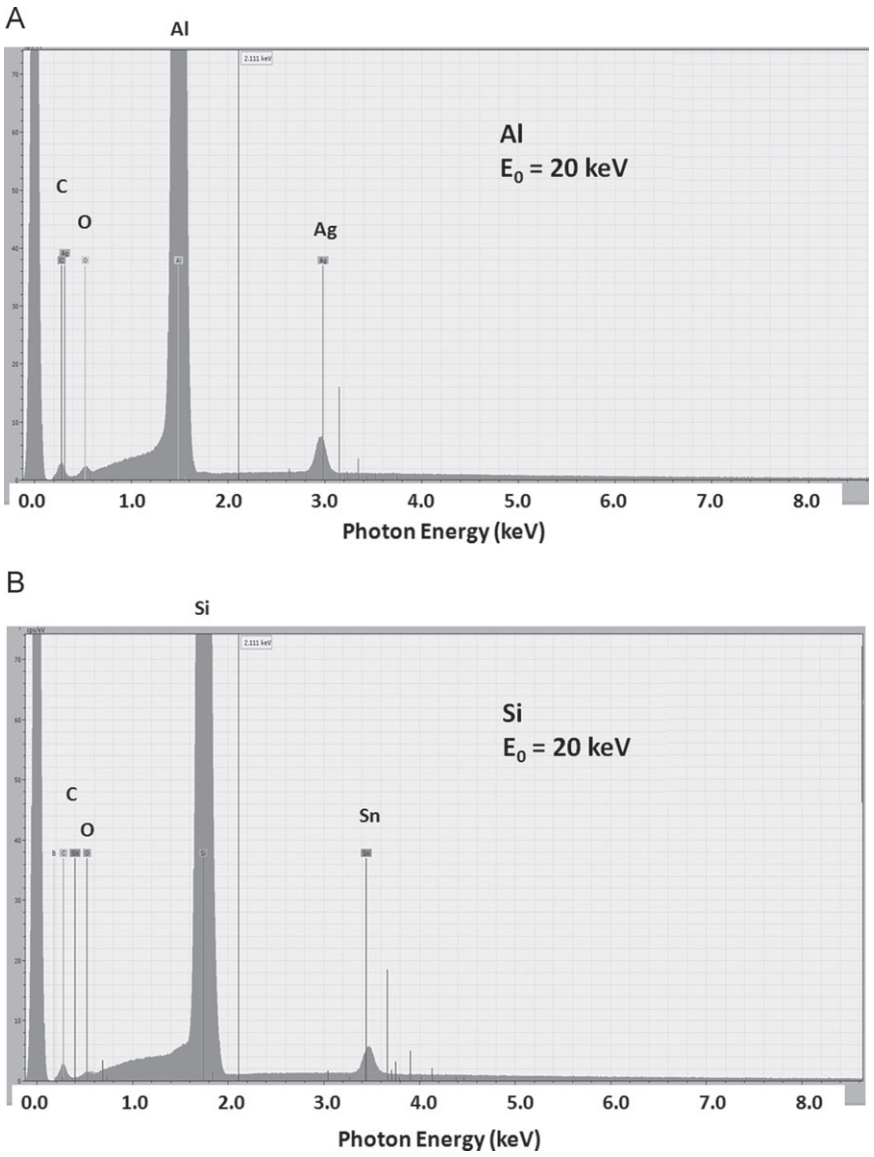

Fig 12. (A) SDD-EDS spectrum of Al with a beam energy of 20 keV showing misidentification of the Al coincidence peak as AgL. (B) SDD-EDS spectrum of Si with a beam energy of 20 keV showing misidentification of the Si coincidence peak as SnL.

measurement. The standardless analysis protocol only requires the list of elements to be analyzed, which is typically and often automatically supplied by the peak identification software, the incident beam energy and the emergence angle of the X-rays above the surface (the so-called X-ray "takeoff" angle). Based upon libraries of stored information, the relative X-ray intensities of the various elemental peaks are converted into relative concentrations and these values are scaled to unity (100 weight%), often with oxygen calculated indirectly by the method of assumed stoichiometry of the cations rather than measured directly. Scaling to unity is needed to put the final values on a sensible basis, a direct requirement because of the loss of electron dose information correlated between the actual measurement conditions and the reference database. Thus, the analytical total in standardless procedures must inevitably total unity, even if a major constituent is inadvertently lost from the qualitative analysis. Two distinct classes of "standardless" analysis exist: (1) "first principles" and (2) "remote standards." Newbury *et al.* ('95) examined both classes of standardless analysis in a study that involved quantitatively analyzing a suite of known materials, including NIST Standard Reference Materials, Research Materials, binary compounds, and homogeneous alloys and glasses, to develop error histograms for standardless analysis similar to that of Figure 1 for the WDS *k*-ratio protocol and ZAF matrix corrections. In that study, only X-ray peaks with photon energies above 0.93 keV (CuL) were considered, all constituents were present at major or high minor concentrations, and oxygen when present was treated by the method of assumed stoichiometry.

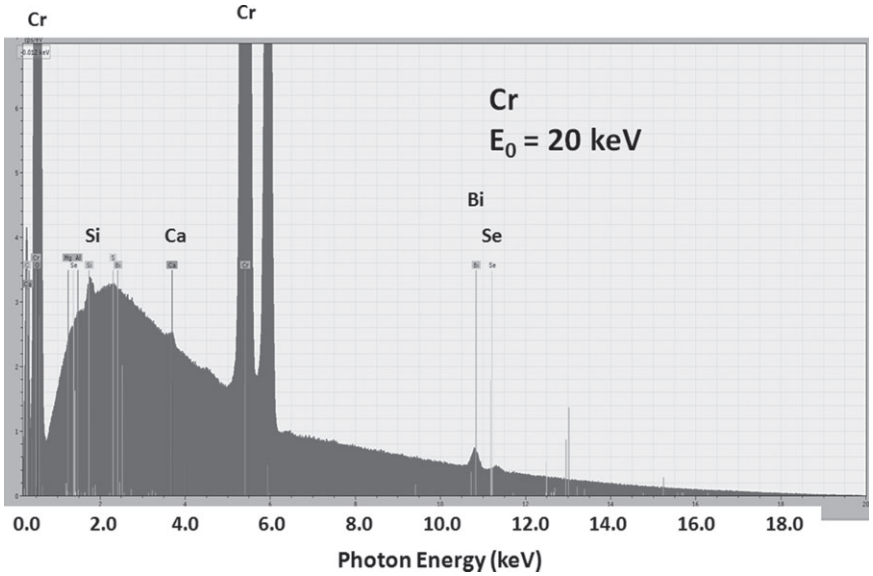

Fig 13. SDD-EDS spectrum of Cr with a beam energy of 20 keV showing misidentification of the Si-escape peak of CrK as CaK and the Cr coincidence peaks as BiL and SeK.

"First principles" standardless analysis

"First principles" standardless analysis uses physical descriptions of the generation, propagation, and detection of X-rays along with databases of physical constants such as ionization cross sections, the depth distribution of ionization, fluorescence yields, mass absorption coefficients, the structure and thickness dimensions of the X-ray detector, etc., to effectively compare intensities of X-ray peaks measured at different photon energies. The accuracy of this method depends greatly on the availability and reliability of many physical constants as well as having an accurate model of the detection efficiency as a function of photon energy, since the efficiency no longer cancels as it does in the *k*-ratio protocol described above. The first principles model (Standardless Miracle) embedded in NIST-NIH Desktop Spectrum Analyzer was examined in the 1995 study and the error histogram shown in Figure 14 was obtained (Newbury *et al.*, '95). This error histogram is roughly symmetrical about zero relative error, but the error bins are 10% relative wide, a factor of ten greater than the scale of the error histogram of Figure 1 for the *k*-ratio protocol with ZAF matrix corrections. The standard deviation of the first principles standardless error histogram is such that the error range spans ±50% relative to capture 95% of the analyses. This broad error range is most likely caused by uncertainties in many of the models and the necessary parameters for X-ray generation, and limitations in modeling the detector efficiency as a function of photon energy. In the *k*-ratio protocol where each characteristic X-ray peak measured for the unknown is compared with the same X-ray peak from a standard, accurate knowledge of the physical basis of X-ray generation is much less important than it is for standardless analysis where different X-ray peaks must be directly compared.

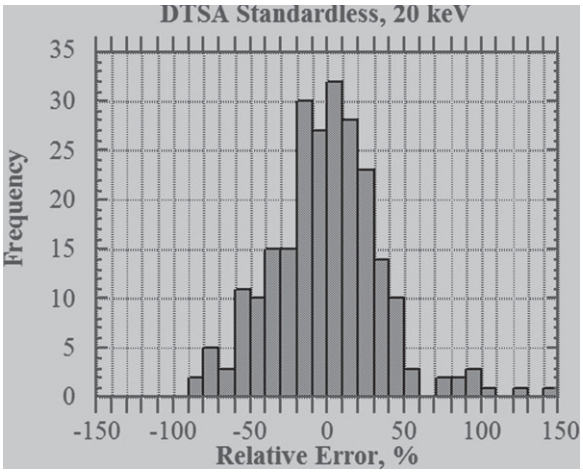

Fig 14. Relative error histogram for a "first principles" standardless analysis protocol ("Standardless Mircacle" in NIST-NIH Desktop Spectrum Analyzer; Newbury *et al.*, '95).

"Remote standards" standardless analysis

Most commercial software implementations of standardless analysis probably follow the "remote standards" protocol ("probably" is used here because these methods are usually "black box" software provided to the user without detailed documentation). Strictly speaking, the "remote standards" protocol is not a true standardless procedure but a method to transfer a carefully measured library suite of standard intensities to the local SEM/EDS measurement environment. The suite of known standards, e.g. pure elements and stoichiometric binary compounds

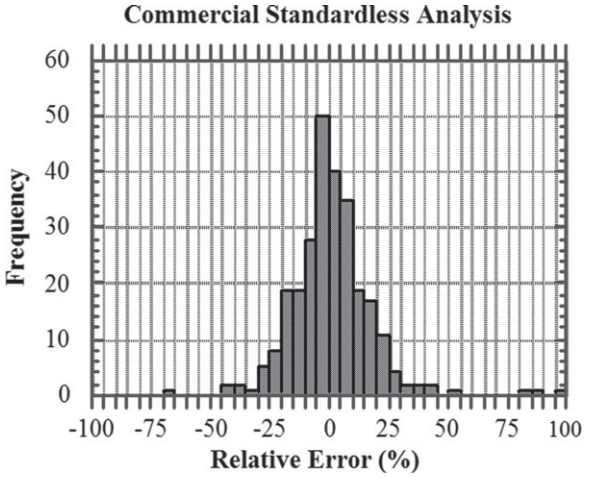

Fig 15. Relative error histogram for a commercial standardless analysis protocol (Newbury *et al.*, '95).

(which are converted by appropriate matrix element calculations into equivalent pure element intensities), is measured at several beam energies and at a consistent dose (beam current × live time) with a well-characterized EDS for which the efficiency as a function of photon energy is known. The resulting database of remotely measured elemental intensities must be adjusted to the local EDS photon efficiency for the particular peak(s) of interest through a detector efficiency transfer calculation usually constrained by a comparison of the X-ray continuum measured on a "pure" continuum spectrum such as that from high-purity carbon, which is minimally affected by the C K characteristic peak. If the local measurement is made with a beam energy different from those represented in the database, then the database standard intensity is adjusted using a model for the energy dependence of X-ray generation constrained by the known values in the database. Similarly, if the standard intensity is required for an element not represented in the database, then the needed value is again estimated with a physical equation for X-ray generation constrained by the measured values for elements with similar atomic numbers. Because the local dose is not taken into account in this method, the analytical total must again be normalized to unity. Figure 15 presents a relative error histogram for a commercial software implementation of "standardless" analysis that was acknowledged by the vendor to follow the remote standards protocol. Again the relative error histogram is approximately symmetrical, but the error bins are a factor of five wider than the error bins in Figure 1. The standard deviation for this remote standards standardless error histogram is such that the error range spans ±25% relative to capture 95% of the analyses.

There is nothing wrong with utilizing a standardless analysis protocol providing the eventual user of the analytical results understands the full implications of the contribution to the measurement uncertainty budget that arises from whatever quantitative analysis protocol is used. However, the error contribution of the quantitative analysis procedure is often not mentioned to the final user of the data because the analyst may be unaware of its magnitude. Commercial standardless analysis software may be supplied without this important information (a careful purchaser would be very wise to ask for this information from a prospective vendor). Instead, the only explicit contribution to the uncertainty budget that is consistently reported is the measurement precision for each element, which is related to the number of X-ray counts accumulated in the characteristic peak of interest and is readily calculable. With reasonable patience by the analyst, the single measurement precision can often be reduced to 0.5% relative or less (i.e., 40,000 counts in the integrated peak above background), in a measurement time of 100 s, especially with the high-throughput SDD-EDS. While achieving excellent measurement precision is important for optimizing the performance of spectral fitting procedures and for comparing measurements at different locations in the specimen, the overall uncertainty budget for the measurement is dominated by the much larger contribution from the quantification method, even in the case of the EDS *k*-ratio/ZAF protocol. Considering the error distribution for "remote standards" standardless analysis in Figure 15, what is the consequence of relative errors in the range ±25% on the utility of final results? Consider that the analyst's problem is to determine the formula of a compound. Table IV gives the results of the analysis of a $YBa_2Cu_3O_{7-x}$ single crystal as performed with the EDS *k*-value/ZAF matrix corrections protocol and with two different commercial standardless analysis procedures, all with oxygen calculated by means of assumed stoichiometry. For the standardless procedures, analysis with CuKα peak as well as with CuL peak was tested. The errors for the three elements were within ±4% relative for the EDS *k*-value/ZAF protocol, which results in the integer formula $YBa_2Cu_3O_{6.8}$ that closely matches the result from independent neutron scattering crystallography measurements. While some of the errors for Ba and Cu with standardless analysis protocols are less than 5% relative, the error for Y is consistently large, with the result that the formulae deduced from the standardless EDS analysis differ significantly from the correct value.

Standardless analysis, both the first principles and remote standards methods, is a subject of intensive continuing research (e.g., Duncumb *et al.*, 2001; Statham 2002, 2006) and there has undoubtedly been much progress since the 1995 study described above. It can be hoped that eventually standardless procedures will match the performance of the EDS

TABLE V Standardless analysis of sulfide minerals with a current commercial standardless analysis protocol (concentrations in mass fraction)

Mineral	Metal	Rel err (%)	S	Rel err (%)	Derived formula
Troilite (FeS)	0.629	−1.1	0.371	+1.8	FeS
Covellite (CuS)	0.764	+15	0.236	−30	Cu_3S_2
Sphalerite (ZnS)	0.762	+14	0.239	−28	Zn_3S_2

k-value/matrix corrections protocol. However, the analyst should not assume that the standardless procedure available in even the latest commercial software is free from the significant errors seen in Figure 15. Table V gives results from a current (2011), recently updated version of a commercial standardless analysis protocol applied to the analysis of metal sulfide minerals. These materials were comounted in the same block and the SDD-EDS spectra were recorded in succession so the performance of the spectrometer was identical during the measurement sequence. The analysis of the meteoritic mineral troilite resulted in sufficiently small errors that the correct formula, FeS, could be deduced from the concentrations. However, the analysis of the minerals covellite (CuS) and sphalerite (ZnS) resulted in such large relative errors that incorrect formulae result. These analytical results are part of an on-going comprehensive study updating the 1995 evaluation by testing current standardless analysis software.

Uncontrolled Specimen Geometry

The third component that leads to questionable EDS analysis, and probably the factor with the highest practical impact on the credibility of quantitative SEM/EDS, is the lack of control of the specimen geometry. As described above, the focusing properties of WDS are so sharply defined that precise positioning of a very flat specimen is necessary for useful, reproducible X-ray intensities to be measured. Deviations from the ideal focus location of only a few micrometers along the optic axis and tens of micrometers laterally cause significant decreases in X-ray intensities. The nonfocusing EDS is not subject to such constraints. Even with a properly mounted collimator, the EDS acceptance volume at the specimen has dimensions of millimeters along all three axes. The volume of transmission for a particular SDD-EDS is shown in Figure 16, where a series of Al X-ray maps taken at positions spaced by 2 mm along the optic axis (for a detector optimized for a 10-mm working distance) are shown, along with a plot of the intensity at the center of each map. Over a total displacement of 1 cm, the center intensity varies by less than 30%, and the lateral variation is generally less than 25% over a displacement of 2 mm. Such a large acceptance volume means that EDS X-ray spectra can be obtained from rough, topographic objects at beam locations where the generation of X-rays is substantially affected by the local specimen topography due to modification of electron penetration and backscattering effects caused by the local thickness and the inclination to the beam. Specimen topography can have even greater impact on the measured X-ray spectrum. The target shape and dimensions can modify the local X-ray absorption path to the detector so that it deviates significantly from the ideal absorption path assumed in the quantification models appropriate to a flat specimen placed at carefully controlled electron-beam incidence and X-ray takeoff angles. The collective result of these complex "geometric effects" is to modify the measured X-ray intensities, often quite substantially, from what would be measured for the ideal flat specimen properly located. One of the basic assumptions of quantitative microanalysis procedures, for both standards-based and standardless procedures alike, is that only composition affects the X-ray intensities. When this condition is violated, very large errors, far exceeding what is expected from an error histogram such as Figure 1 or Figure 15, can occur.

To demonstrate the impact of such geometric factors, a series of tests has been performed on NIST SRM 470 (K411 glass), the composition of which is given in Table VI. K411 provides a range of X-ray energies from the energetic FeKα peak at 6.400 keV, which is relatively unabsorbed to the low-energy MgKα peak at 1.254 keV, which is sensitive to absorption effects. The dispersion of results from analysis with the NIST DTSA-II software engine of K411 in the form of an ideal flat polished specimen is shown in Figure 17. A beam energy of 20 keV was used, and the standards were Mg (element), Si (element), Ca (SRM glass K-412), and Fe (element), and the results were normalized for direct comparison in the following studies. The mean of the 20 measurements lies within +1.8% relative of the SRM value for Fe and −1.0% relative of the SRM value for Mg. Both the Fe and Mg results cluster within a range of approximately 1% relative, with one exception (circled). Considering the concentration precision of the

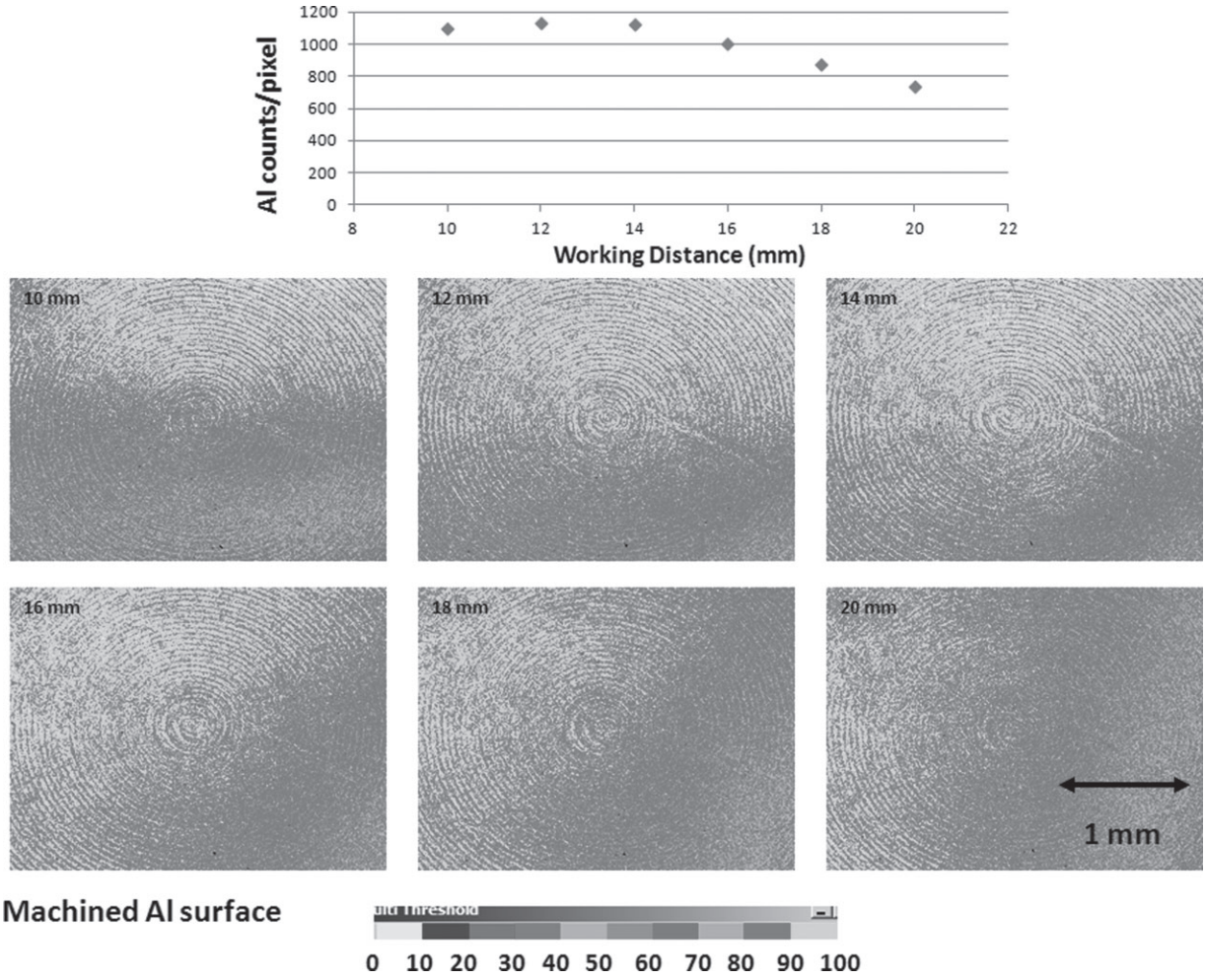

Fig 16. Transmission of an SDD-EDS as measured by X-ray mapping of a machined aluminum disk at successive 2-mm displacements along the optic axis. The intensity measured at the center of each map is plotted.

TABLE VI NIST Standard Reference Material 470 (glass K 411; concentrations in mass fraction)

Element	SRM certificate value	Kα energy (keV)
O	0.4236	0.523
Mg	0.0885	1.254
Si	0.2538	1.740
Ca	0.1106	3.690
Fe	0.1121	6.400

individual measurements, indicated in Figure 17 by the arrows (upper right), this circled point is clearly sufficiently outside the cluster to identified as anomalous and may represent a local inhomogeneity, which is actually quite rare in these materials (Marinenko *et al.*, '79). A second and more likely possibility is that this point represents a measurement inadvertently made at the site of a surface topography flaw (see below).

Effect of surface finish

Similar to the study performed by Yakowitz ('68), the specimen of NIST SRM 470 (glass K411) was subjected to surface roughening with a "1-μm diamond polish," recoated with ~7 nm of carbon, and reanalyzed under the same conditions as used for the ideal flat polished specimen. Both sets of results are plotted in Figure 18, where the effect of the modest surface roughness is seen to expand the size of the cluster and shift it significantly. The magnitude of the shift due to the scratches suggests that the anomalous point in Figure 17 might arise from a surface scratch that was inadvertently sampled by the automatic randomization of measurement points.

Effect of more severe topography

Figure 14 shows an SEM image (inset) of a more severe surface defect induced in polished K-411 glass by mechanical abrasion with 600 grit SiC. EDS spectra are readily obtainable from any beam location within this topographic feature, and the normalized Mg and Fe concentrations have a much greater range, as shown in Figure 19, compared to the values for ideal flat polished specimen, which reside within the box. The apparent concentration range now spans

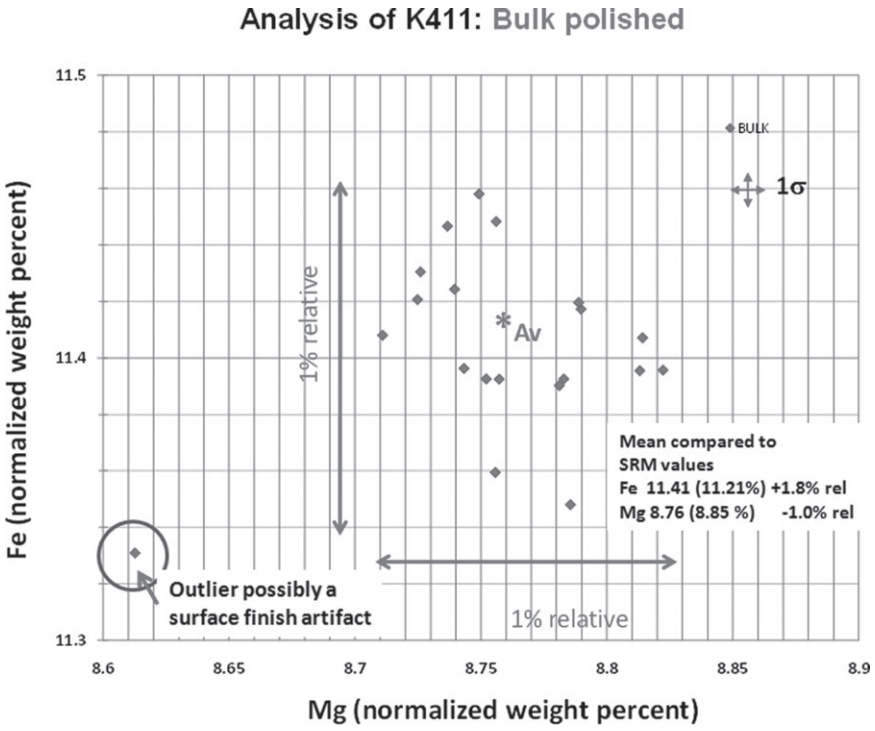

Fig 17. Dispersion of the Mg and Fe concentrations from the analysis of NIST SRM 470 (glass K411) in the ideal flat, polished form. Beam energy = 20 keV. $1-\sigma$ counting statistics expressed as a concentration uncertainty are shown. Note outlier point (circled; Newbury and Ritchie, 2011).

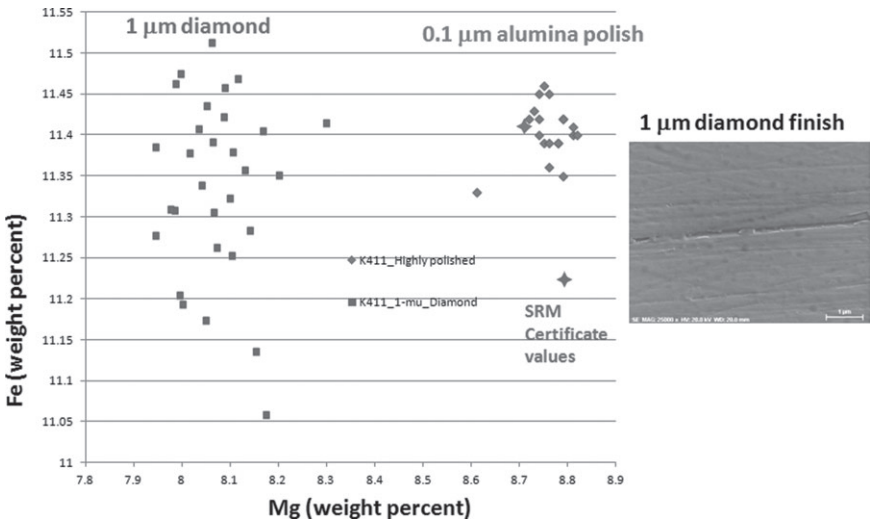

Fig 18. Dispersion of the Mg and Fe concentrations from the analysis of NIST SRM 470 (glass K411) after abrasion with "1-μm diamond" polish (Newbury and Ritchie, 2011).

an order of magnitude for Mg and a factor of three for Fe.

This study was extended to include additional specimen geometries, including deep surface holes, microscopic particles, and macroscopic fragments, examples of which are shown in Figure 20. The summary of the Mg and Fe concentration results is shown in Figure 21, in which the concentration range for Mg spans a factor of 40 and that for Fe spans a factor of ten.

Diagnostics of geometric effects on quantitative analysis

Shape of the X-ray continuum. There are obvious indications of the impact of geometric effects on quantitative analysis, which the careful analyst can observe. Figure 22 shows selected examples of the K-411 spectra from various locations on macroscopic shards. Compared to the polished flat, bulk K-411, the shard spectra show very pronounced deviations in the shape of the X-ray continuum background below a photon energy of approximately 5 keV. It is worth noting that

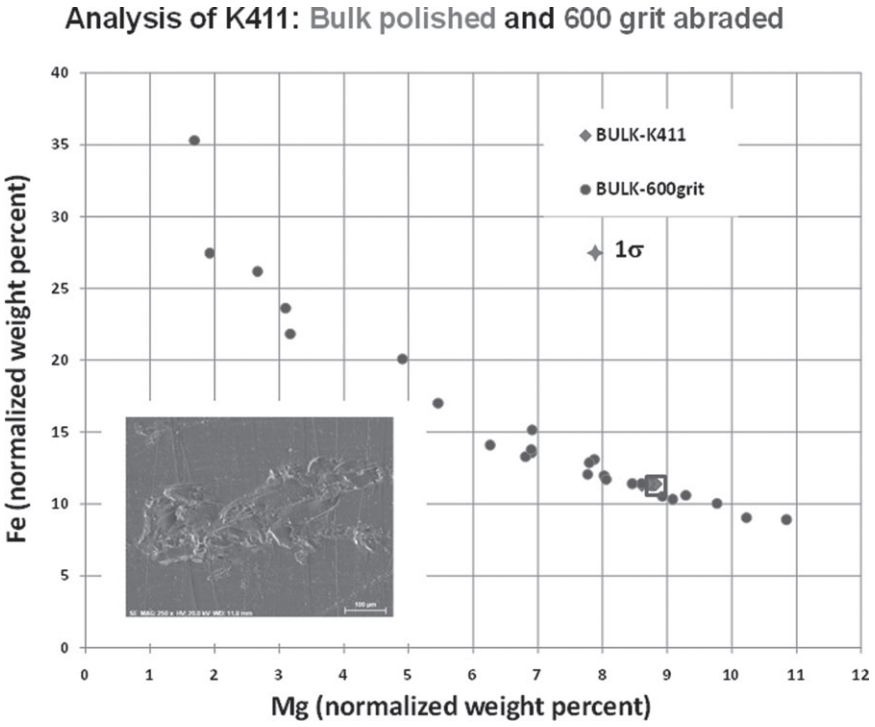

Fig 19. Dispersion of the Mg and Fe concentrations from the analysis of NIST SRM 470 (glass K411) after more severe abrasion with "600 grit" SiC and SEM image (Everhart-Thornley detector, positively biased to collect secondary electrons) of the surface (Newbury and Ritchie, 2011).

many of the low-energy photon energy characteristic peaks are present in these spectra, except for the most extreme case, although the peak intensities are attenuated, in most cases severely. For an unknown it is not possible to assess *a priori* the possible impact of geometric effects from the characteristic peaks, since these intensities obviously scale strongly with concentration, but the shape of the X-ray continuum over a wide, low photon energy range does embed this topographic information. Indeed, advanced correction methods for topographic effects are based upon measurements of the peak-to-local-background (Small *et al.*, '78; Statham and Pawley, '78). By studying the shape of the EDS spectra from flat, bulk targets, the analyst can develop a good idea of the proper spectrum shape. Alternatively, spectrum synthesis tools, such as those available in DTSA-II can be used to calculate the spectrum of hypothetical compositions for comparison to measured spectra. An example of such a calculation for flat bulk K-411 is shown in Figure 23, demonstrating that a good correspondence can be achieved between measurement and a theoretical prediction that considers absolute dose and EDS solid angle.

Raw analytical total. A second strong indicator of the severity of geometric effects is the raw analytical total that is obtained when analysis is performed with the EDS *k*-ratio/matrix corrections protocol with flat polished standards. Figures 24(A) and (B) show the Mg and Fe concentrations plotted against the raw analytical total for the analysis. Note that totals below and above 100% are observed, a result of the complex effects of specimen geometry on electron scattering and the X-ray absorption path. As long as the raw analytical lies within 80–120% for these particular elements in this particular overall composition, the relative errors for Mg and Fe lie within approximately ±20% relative. While this is still a large systematic error range, the error values are at least within an acceptable range for some applications, and the raw analytical total is a good indicator of the likelihood of more severe errors. The useful information provided by the raw analytical total is of course lost in the standardless analysis protocols because the absence of dose and detector solid angle information leads to the inevitable requirement for normalization.

Performing Accurate SEM/EDS Analysis

The EDS system can record apparently credible spectra from virtually any location on the objects shown in Figure 20. Unfortunately, the concentration results from these spectra reported in Figure 21 are subject to such great systematic errors as to be of little use for virtually any practical application, even

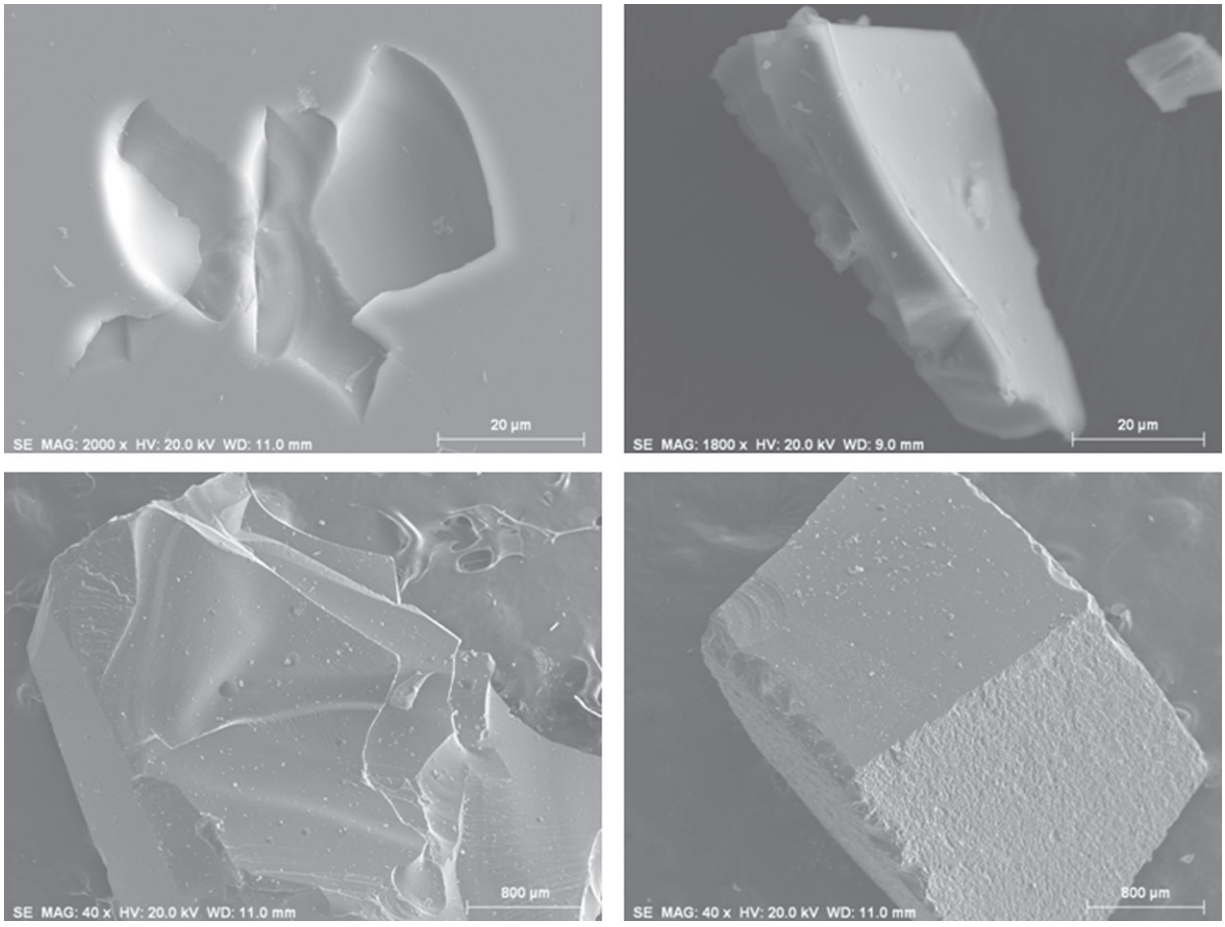

Fig 20. SEM images (Everhart-Thornley detector, positively biased to collect secondary electrons) of the various topographic features created with NIST SRM 470 (glass K-411; Newbury and Ritchie, 2011).

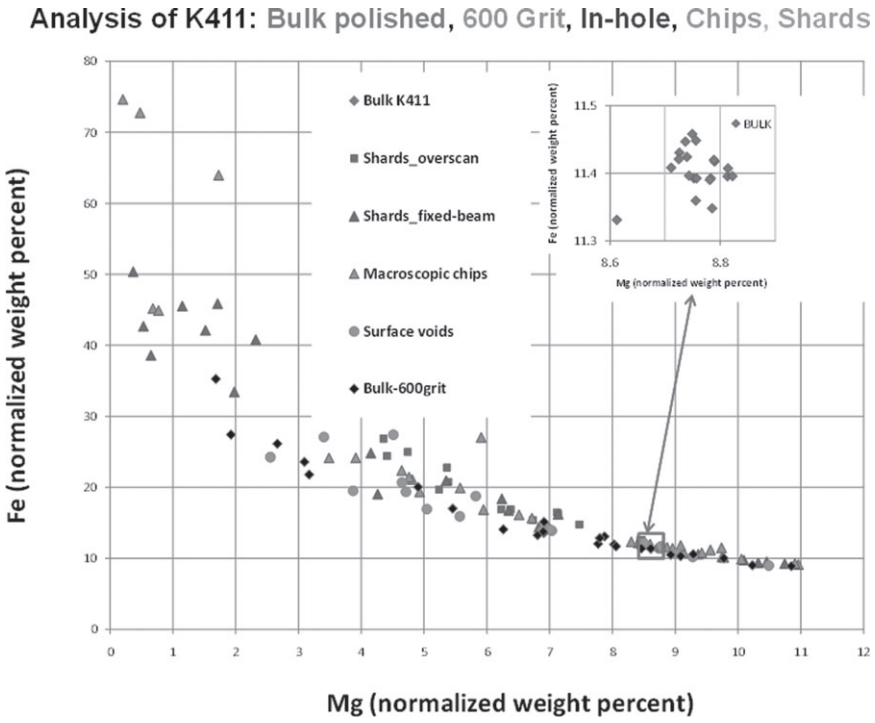

Fig 21. Plot of Mg and Fe concentrations analyzed for NIST SRM 470 (glass K-411) in all of the specimen topography forms tested (Newbury and Ritchie, 2011).

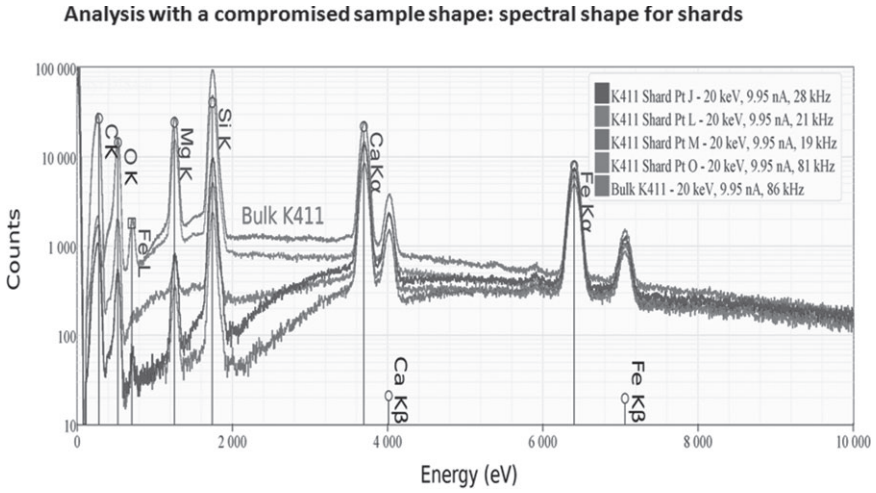

Fig 22. Comparison of spectra of K-411 glass from flat polished bulk and from shards of various sizes (Newbury and Ritchie, 2011).

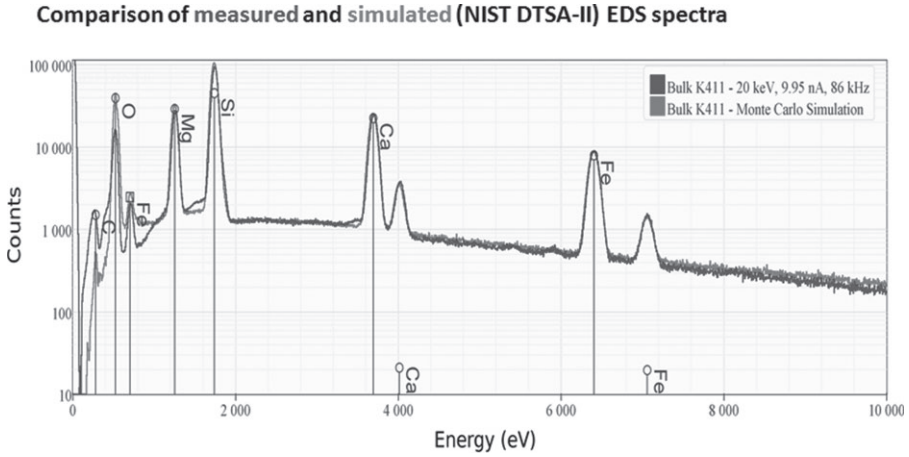

Fig 23. Comparison of K-411 spectra as measured and as simulated with NIST DTSA-II; absolute calculation based upon electron dose and SDD-EDS solid angle (Newbury and Ritchie, 2011).

broadly classifying the results into major, minor, and trace categories. The large acceptance volume of the EDS simply makes it too easy to record spectral information that is severely compromised by specimen geometry effects. As commonly practiced throughout the microanalysis community, standardless analysis will then convert those severely compromised spectra into severely compromised elemental concentrations, which will nevertheless add up to unity and which, with modest patience during spectrum accumulation, can be accompanied by a precision estimate that may be well below 1% relative, giving false hope to the unwary. With such poor measurement science taking place, it should therefore not be surprising that SEM/EDS standardless quantitative microanalysis has a poor reputation compared to quantitative WDS quantitative microanalysis with standards and ZAF/$\phi(\rho Z)$ matrix corrections, which by its very nature demands rigorous measurement science and for which the raw analytical total provides a strong indication of deviations from proper measurement conditions.

This unfortunate situation does not have to exist. As demonstrated by the results presented in Table I, it has been possible for at least 30 years to obtain highly reliable, quantitative microanalyses with EDS by following the *k*-ratio measurement protocol with the same care and rigor as is commonly done for WDS *k*-ratio measurements. With the advent of SDD-EDS, precision and accuracy comparable to that of WDS can be obtained with the *k*-ratio protocol, even for severe peak overlaps.

The procedure to achieve high-reliability quantitative X-ray microanalysis by SEM-EDS has the following steps:

1. Use carefully prepared unknowns and standards polished to a surface roughness below 50 nm, and preferably below 20 nm if characteristic peaks with photon energies below 1 keV are to be

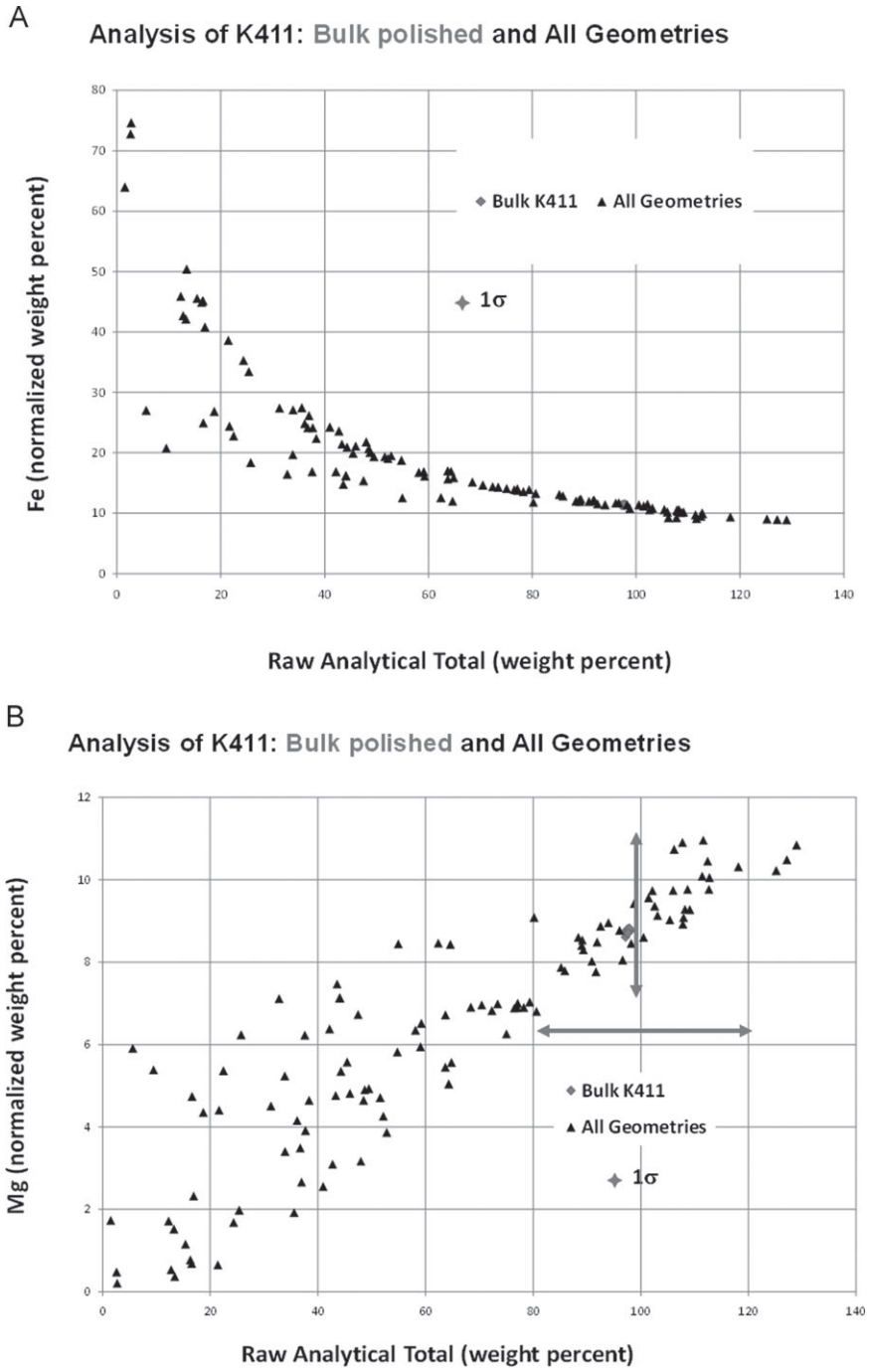

Fig 24. (A) Normalized concentration of iron versus the raw analytical total for K-411 in various geometric forms. The vertical arrow emphasizes the range of Fe-concentration that occurs within the span of the horizontal arrow, which covers an analytical total between 80% and 120% (Newbury and Ritchie, 2011). (B) Normalized concentration of magnesium versus the raw analytical total for K-411 in various geometric forms. The vertical arrow emphasizes the range of Mg-concentration that occurs within the span of the horizontal arrow, which covers an analytical total between 80% and 120% (Newbury and Ritchie, 2011).

analyzed. (The polished surface should not be chemically etched, since etching can substantially modify the near-surface composition that is sampled by electron-excited X-ray spectrometry.)

2. Measure the unknowns and standards under controlled, reproducible electron dose as confirmed by repeated specimen current measurements during the analytical campaign. (A stage Faraday cup and a high-performance picoammeter to unambiguously measure beam current are indispensable tools for establishing high-quality standards-based quantitative analysis.) If a beam current measurement is not possible, then the integrated full-spectrum intensity of a standard repeatedly

measured during the measurement sequence can be used for an internal normalization if the beam current drifts.

3. Measure the unknowns and standards with consistent specimen positioning to maintain a consistent detector takeoff angle and detector solid angle. To achieve this condition in an SEM environment that lacks a positioning aid, such as the fixed-focus optical microscope of the EPMA, for precise location of the specimen along the optic axis relative to the X-ray detector, the unknowns and standards should be comounted so that only lateral translation is required to move between them.
4. Establish a quality assurance protocol for EDS operation that includes regular energy calibration and consistent choice of user-selectable software parameters (e.g., time constant, energy per channel) and hardware parameters (e.g., adjustable EDS position).
5. The strategy for optimum EDS operation must be carefully considered. As demonstrated above, it is very desirable to record high-count spectra of standards and unknowns to enable accurate and precise measurement of characteristic peak intensities. To obtain such high counts, it is tempting to operate at high dead time to maximize spectral counts per unit of clock time, but as shown in Figure 6, the ingrowth of coincidence peaks as a function of dead time creates a serious artifact that compromises accurate measurement of the parent peak(s) as well as possibly interfering with peaks of minor/trace constituents. The proper dead time to use depends on the particular detector, but a conservative counting strategy would be to choose a beam current for the particular detector solid angle that yields a maximum dead time of ~25% for Si(Li)-EDS and ~10% for SDD-EDS on the most highly excited standard or unknown. This particular beam current/EDS solid angle combination should then form the basis for future measurements if a library of archived standards is to be established.
6. For quantitative analysis, choose the EDS *k*-ratio protocol with MLLS intensity measurement of the *k*-ratio followed by matrix corrections that is available in virtually all commercial microanalysis software systems. If the software provides access to more than one matrix correction schemes, seek to understand their relative strengths and weaknesses so as to make the optimal choice for the particular suite of elements under examination. For a more complete examination of the impact of the choice of the matrix correction model, the CITZAF software engine of Armstrong (1995) provides a comprehensive collection of the available matrix correction procedures. The user can take the set of *k*-values determined by his/her local commercial software engine and input these *k*-values to the CITZAF engine to examine the dispersion of calculated concentration values that result from virtually all possible models.
7. The analytical total from the *k*-value/matrix correction procedure provides valuable information and should be examined for every analysis. Deviations from a mass fraction total of unity can reveal a missing element as well as the operation of unexpected geometric factors or pathological effects, such as contamination layers. If the analyst chooses to use a standardless analysis procedure, the analytical total is lost as a tool.
8. It is incumbent on the analyst who chooses to use standardless analysis to seek to understand the systematic error distribution that the particular procedure produces. If this information is not available from the originator of the procedure, then the analyst must assess the systematic errors by testing known materials of similar composition to the unknowns. Otherwise, it is prudent to assume that the error distribution is probably similar to that shown in Figure 15 rather than that shown in Figure 1.
9. The commercial quantitative analysis program will certainly provide some measure of the precision. The analyst should seek to understand what statistical measure is reported. Goldstein *et al.* (2003) provide an explicit calculation of the standard deviation of the concentration value, σ_C, taking into account the four sources of variance in the *k*-ratio measurement (the characteristic peak count and the background count for both the unknown in the numerator of the *k*-ratio and for the standard in the denominator). This value of σ_C enables determination of a confidence interval around the calculated concentration value for each element.

Conclusion

Is SEM/EDS quantitative? The answer can be a resounding Yes! Quantitative EDS analysis following the *k*-ratio protocol can match WDS for the accuracy and precision with which the characteristic X-ray intensities are measured with a dose that is lower by a factor of 3–60 depending on the particular instrument configuration, even when severe peak overlap occurs and a large concentration ratio (>20:1) exists for the mutually interfering peaks. When these *k*-ratios are subjected to matrix corrections to determine concentration values, the results show a distribution of relative errors such that a conservative estimate is that 95% of the concentrations fall within ±5% relative of the correct value. However, there are no shortcuts to the protocol that can be made without compromising this performance. The measurement rigor demanded by the *k*-ratio protocol must be carefully followed,

including the preparation of a highly polished surface for the unknowns and standards and control of all measurement parameters to ensure that the intensities determined for the unknown and the standard(s) are measured under identical (or scalable) conditions.

Unfortunately, SEM/EDS is vulnerable to at least three significant measurement challenges that can severely degrade the analytical results. (1) Automatic peak identification software can occasionally misidentify even major peaks, and the frequency of misidentification increases as the concentration levels decrease from major to minor to trace. The careful analyst will always confirm the peak identification suggested by the automatic software before proceeding to perform quantitative analysis. (2) Standardless quantitative analysis procedures can produce useful concentration values, but the distribution of relative errors for standardless techniques is generally broader than that for the *k*-ratio/matrix correction protocol by a factor as high as five. Such an error distribution is still useful as long as the user of the analytical results is provided with a proper error budget that includes an estimate of the precision from the counting statistics of the various measured intensities and an estimate of the systematic error from the performance of the matrix correction method, which determines accuracy. (3) The ease with which EDS spectra can be measured from rough objects with complex topography frequently leads analyses of spectra from specimen locations which may be severely compromised by large modifications to the electron scattering, X-ray generation, and X-ray propagation as compared to a flat, bulk target placed at known angles to the beam and the EDS. The resulting systematic errors introduced by geometric effects can be orders of magnitude greater than the errors associated with quantification by either *k*-ratio/matrix correction procedures or standardless analysis.

Despite the increasing level of sophistication of the software tools that support EDS X-ray microanalysis, which are now often advertised as being capable of one button operation for elemental identification and quantification with results written directly to a report, such automatic analysis cannot yet replace the understanding, critical interpretation, and experience brought to EDS microanalysis problem solving by the analyst. A major conclusion of this article is to assert the vital requirement that the analyst must consider the computer-aided analysis software only as a set of tools to be used with extreme care while recognizing his/her responsibility to properly interpret the results for the final report. Thus, it is critical to understand the limitations of performance of EDS microanalysis and not surrender to the apparent authority of the result on the computer screen or written directly into an elaborate report.

References

Armstrong JT. 1995. CITZAF: a package of correction programs for the quantitative electron microbeam X-ray analysis of thick polished materials, thin films and particles. Microb Anal 4:177–200.

Castaing R. 1951. Applications of electron beams to a method of local chemical and crystallographic analysis. Paris: University of Paris.

Currie LA. 1968. Limits for qualitative detection and quantitative determination. Anal Chem 40:586–593.

Duncumb P, Barkshire I, Statham P. 2001. Improved X-ray spectrum simulation for electron microprobe analysis. Microsc Microanal 7:341–355.

Fiori CE, Myklebust RL, Heinrich KFJ, Yakowitz H. 1976. Prediction of continuum intensity in energy-dispersive X-ray microanalysis. Anal Chem 48:172–176.

Fiori CE, Swyt CR, Myklebust RL. 1992. Desktop spectrum analyzer (DTSA), a comprehensive software engine for electron-excited X-ray spectrometry. National Institute of Standards and Technology (NIST)—National Institutes of Health (NIH), United States, Patent 5,299,138 (March 29, 1994). Gaithersburg, MD: Standard Reference Data Program, NIST.

Fitzgerald R, Keil K, Heinrich K. 1968. Solid-state energy-dispersion spectrometer for electron-microprobe X-ray analysis. Science 159:528–530.

Goldstein JI, Newbury DE, Joy DC, Lyman CE, Echlin P, Lifshin E, Sawyer L, Michael J. 2003. Scanning electron microscopy and X-ray microanalysis. 3rd ed. New York: Springer.

Lifshin E, Ciccarelli MF, Bolon RB. 1975. X-ray spectral measurement and interpretation. In: Goldstein JI, Yakowitz H, Newbury DE, Lifshin E, Colby JW, Coleman JR, editor. Practical scanning electron microscopy. New York: Plenum. p. 263.

Marinenko RB, Heinrich KFJ, Ruegg FC. 1979. Microhomogeneity of NBS standard reference materials, NBS research materials, and other related samples, NBS special publication 260–65. Washington, DC: U.S. Department of Commerce/National Bureau of Standards.

Myklebust RL, Fiori CE, Heinrich KFJ. 1979. FRAME C: a compact procedure for quantitative energy-dispersive electron probe X-ray analysis. National Bureau of Standards Technical Note 1106. Washington, DC: National Bureau of Standards.

Newbury DE. 2000. Energy-dispersive spectrometry. In: Kaufmann EN et al., editor. Methods in materials research. New York: John Wiley & Sons. p 11d.1.1–11d.1.25

Newbury DE. 2005a. X-ray spectrometry and spectrum image mapping at output count rates above 100 kHz with a silicon drift detector on a scanning electron microscope. Scanning 27:227–239.

Newbury DE. 2005b. Misidentification of major constituents by automatic qualitative energy dispersive X-ray microanalysis: a problem that threatens the credibility of the analytical community. Microsc Microanal 11:545–561.

Newbury DE. 2007. Mistakes encountered during automatic peak identification in low beam energy X-ray microanalysis. Scanning 29:137–151.

Newbury DE. 2009. Mistakes encountered during automatic peak identification of minor and trace constituents in electron-excited energy dispersive X-ray microanalysis. Scanning 31:1–11.

Newbury DE, Ritchie NWM. 2011. Is scanning electron microscopy/energy dispersive X-ray spectrometry (SEM/EDS) quantitative? Effects of specimen shape. SPIE Proc 8036:803601-1–803602-16.

Newbury DE, Swyt CR, Myklebust RL. 1995. 'Standardless' quantitative electron probe microanalysis with

energy-dispersive X-ray spectrometry: is it worth the risk? Anal Chem 67:1866–1871.

Pouchou J-L, Pichoir F. 1991. Quantitative analysis of homogeneous or stratified microvolumes applying the model "PAP." In: Heinrich KFJ, Newbury DE, editors. Electron probe quantitation. New York: Plenum. p 31.

Reed SJB, Ware NG. 1972. Escape peaks and internal fluorescence in X-ray spectra recorded with lithium drifted silicon detectors. J. Phys. E: Sci. Inst. 5:582–583.

Ritchie NWM. 2011. Standards-based quantitfication in DTSA-II—part 1. Microsc Today 19:30–36.

Ritchie NWM, Newbury DE, Davis J. 2012. EDS measurements of X-ray intensity at WDS precision and accuracy using a silicon drift detector. Microsc Microanal. In press.

Schamber FC. 1973. A new technique for deconvolution of complex X-ray energy spectra. In: Proc. 8th National Conference on Electron Probe Analysis. New Orleans, LA: Electron Probe Analysis Society of America. p 85.

Small JA, Heinrich KFJ, Fiori CE, Myklebust RL, Newbury DE, Dillmore MF. 1978. The production and characterization of glass fibers and spheres for microanalysis. Scanning Electron Microsc. 1978 I:445–454.

Statham P. 2002. Limitations to accuracy in extracting characteristic line intensities from X-ray spectra. J Res Natl Inst Stand Technol 107:531–546.

Statham P. 2006. Pile-up correction for improved accuracy and speed of X-ray analysis. Microchim Acta 155:289–294.

Statham PJ, Pawley JB. 1978. A new method for particle X-ray micro-analysis based on peak to background measurements. Scanning Electron Microsc I:469–478.

Struder L, Fiorini C, Gatti E, Hartmann R, Holl P, Krause N, Lechner P, Longoni A, Lutz G, Kemmer J, Meidinger N, Popp M, Soltau H, van Zanthier C. 1998. High resolution non dispersive X-ray spectroscopy with state of the art silicon detectors. Mikrochim Acta Suppl 15:11–19.

Yakowitz H. 1975. Methods of quantitative analysis. In: Goldstein JI, Yakowitz H, Newbury DE, Lifshin E, Colby JW, Coleman JR, editors. Practical scanning electron microscopy. New York: Plenum. p 338.

Yakowitz H. 1968. Fifty years of progress in metallographic techniques, ASTM—special technical publication 430, Vol. 430. Philadelphia, PA: American Society of Testing and Materials. p 383.